

Politecnico di Torino



Petroleum Engineering Master's Degree Thesis
Wellbore stability in bedded formation

Advisor:

Prof.ssa Chiara Deangeli

Candidate:

Federico Stoppelli

Academic year 2018/19

Summary

Introduction.....	5
Chapter 1.....	6
Fundamentals of Geomechanics.....	6
1.1 State of stress.....	6
1.2 Equilibrium equations.....	7
1.3 Strain.....	8
1.4 Compatibility equations and solution.....	9
1.4.1 Elasticity and Hooke's law.....	10
1.5 Plasticity.....	12
1.6 Essentials of strength criteria.....	13
1.6.1 Mohr-Coulomb criterion.....	13
1.6.2 Hoek & Brown empirical criterion.....	15
1.6.3 Griffith model.....	16
1.7 Anisotropy rocks.....	17
1.7.1 Plane of weakness model.....	17
1.8 Terzaghi Principle.....	19
Chapter 2	21
STRESS AROUND BOREHOLE.....	21
2.1 Cylindrical coordinates.....	21
2.2 Stresses and strains.....	21
2.3 Hints about State of stress for anisotropic conditions.....	23
Chapter 3	26
Modelling of Wellbore stability in transverly isotropic formation.....	26

3.1	<i>Fast Lagrangian analysis of Continua (FLAC) implementation</i>	27
3.2	<i>Formation parameters</i>	28
3.2.1	<i>Posedonia shale</i>	29
3.2.2	<i>Opalinus clay</i>	30
3.3	<i>FLAC METHODOLOGY</i>	32
	<i>Chapter 4</i>	36
	<i>SIMULATION RESULTS</i>	36
4.1	<i>Opalinus Clay failure simulation</i>	36
4.1.1	<i>Undrained conditions process simulation</i>	36
4.1.2	<i>Drained conditions process simulation</i>	36
4.2	<i>Posedonia Shale Failure Simulation</i>	45
4.2.1	<i>Undrained conditions process simulation</i>	45
4.2.2	<i>Drained conditions process simulation</i>	50
4.3	<i>Discussion of the results</i>	51
5.1	<i>CONCLUSIONS</i>	53
	<i>APPENDIX A</i>	54
	<i>APPENDIX B</i>	57
	<i>REFERENCES</i>	60

Acknowledgements

*“A long journey consists of many steps,
each of these was accompanied by people who enriched it”*

I thank my Mother who has never influenced my choices.
I thank my sisters and brothers without whom I could not have even taken the initial step.

To my friends:

Adele, Alessia, Benedetta, Elena, Francesco & Michele who supported me, endured and
rejoiced.

To all those people who, even if for a while, have gladdened this journey.

A special thanks to my supervisor, prof.ssa Chiara Deangeli, whose infinite availability helped
me to develop this work.

Introduction

In the oil and gas industry, one of the principal step in the development of a reservoir is drilling well that permit us to take off petroleum from the subsurface.

The wellbore construction is one of the most critical process that involves a different kind of workers such as geologists, geophysicists, drilling engineers, drilling fluids engineers which collect all the information useful to drill a stable wellbore and how to maintain it during the production life of the reservoir.

To make decision on the drilling process, the drilling engineers must know how the formation is characterized, which kind of drilling bit use, which kind of mud use to sustain the wellbore walls (density) and all the petrophysical parameters of the formation.

The issue in the drilling process is the stability of the wellbore. During the drilling process and before the wellbore become cemented, the wall could fail and break. This is a critical situation that should not occur.

Formation, obviously, are not homogeneous and the properties change in the different points of the formation. Thanks to the sedimentation process, to the erosion, to the compaction during eras, formations undergo changes in shape and lithology. This makes possible the formation of planes along which the properties have value smaller than the entire block of rock. This particular situation is called: weakness plane model and it is the main task of this thesis.

The aim of this thesis is to study the behaviour of two different formations, characterized by weakness plane, when a wellbore is drilled in them, and how the stability changes with varying the inclination of bedding planes.

The formations analysed are the Posedonia shale and the Opalinus clay.

Fundamentals of Geomechanics

1.1 State of stress

Within a generic volume of rock we can define two kind of forces: body force (associated with the mass of the rock itself) and surface force (associated to the physical contact between the bodies[1] .

In a generic point of a rock body, the state of stress is characterized by 9 components of stress of which 6 are independents[1] (fig 1).

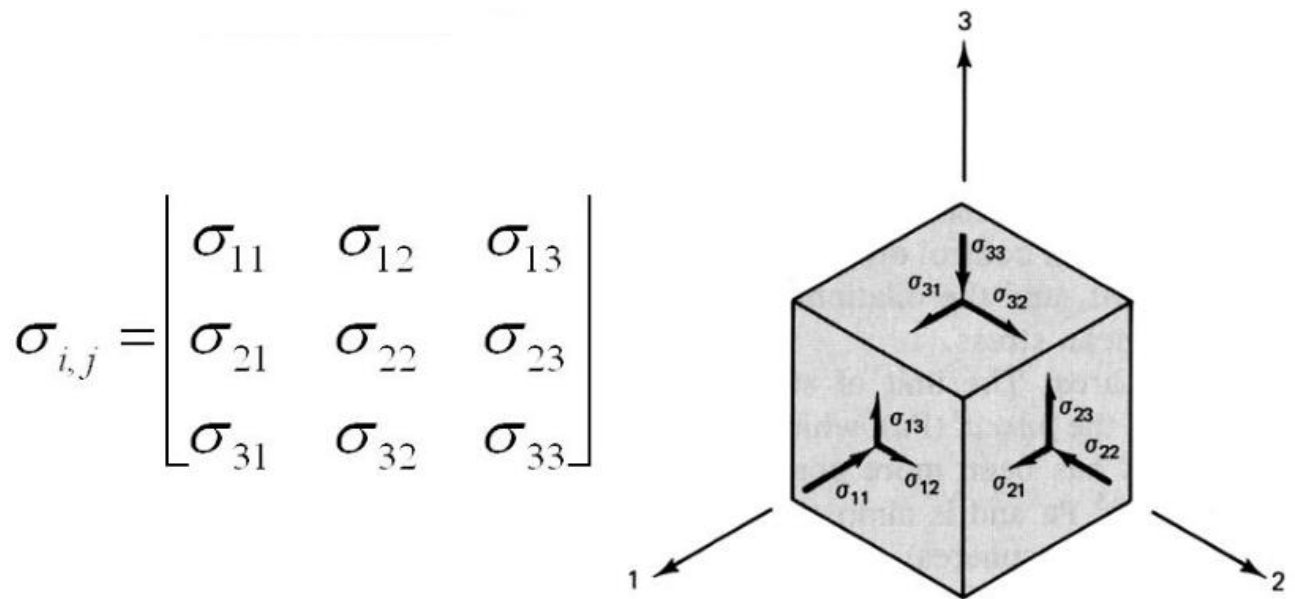


Fig 1.1 : state of stress in a point and stress tensor[1]

The state of stress can be represented graphically through the Mohr's circle, in which are present all the possible states of stress of a body with respect to the different orientations of it. The utility of this method lies on the fact that it permits us to visualize immediately the relation between shear stress and normal stress, and help us to calculate the stress on various inclined planes and the principal stresses[1] .

Mohr's Circle can be drawn down for both 2D and 3D geomechanics models.

An example is attached below (fig 1.2):

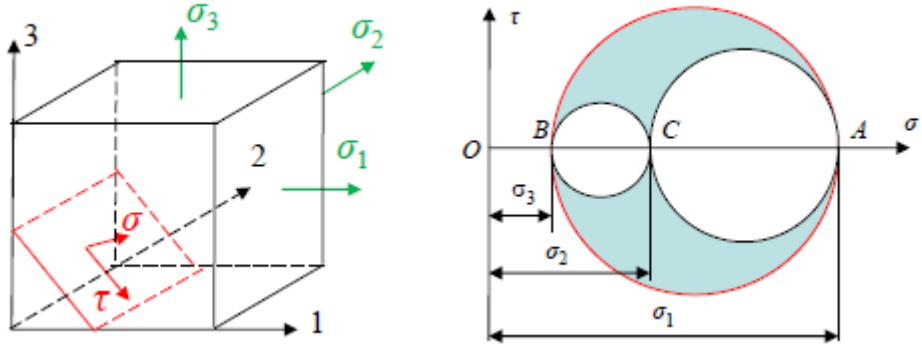


Fig1.2: Mohr circle for 3D model [11]

1.2 Equilibrium equations

On a body not only surface forces and body forces are acting, there are other forces that must be consider during the analysis of the state of stress[1] .

The overburden, the presence of water, the state of preconsolidation and compaction are some of the causes of these other forces. During the study of the static equilibrium all these different contribution must be added and make an important effect on the state of stress of the body[1].

The equilibrium equations are written for the three dimensions[1] :

$$\frac{\delta\sigma_x}{\delta x} + \frac{\delta\tau_{xz}}{\delta y} + \frac{\delta\tau_{xy}}{\delta z} + X = 0 \quad (1.1)$$

$$\frac{\delta\sigma_y}{\delta y} + \frac{\delta\tau_{yz}}{\delta z} + \frac{\delta\tau_{xy}}{\delta x} + Y = 0 \quad (1.2)$$

$$\frac{\delta\sigma_z}{\delta z} + \frac{\delta\tau_{xz}}{\delta x} + \frac{\delta\tau_{zy}}{\delta y} + Z = 0 \quad (1.3)$$

But these equations aren't enough to describe completely the state of stress of a body, because the unknowns are more then the known parameters: we need other relations to figure out the problem.

1.3 Strain

The state of stress makes an important effect of the deformation of a body. The state of strain considers all the change in shape and volume of a rigid body through infinitesimal analysis of the forces acting on it.

There are two types of strain: elongation ϵ , and shear strain Γ (fig1.3) [1]:

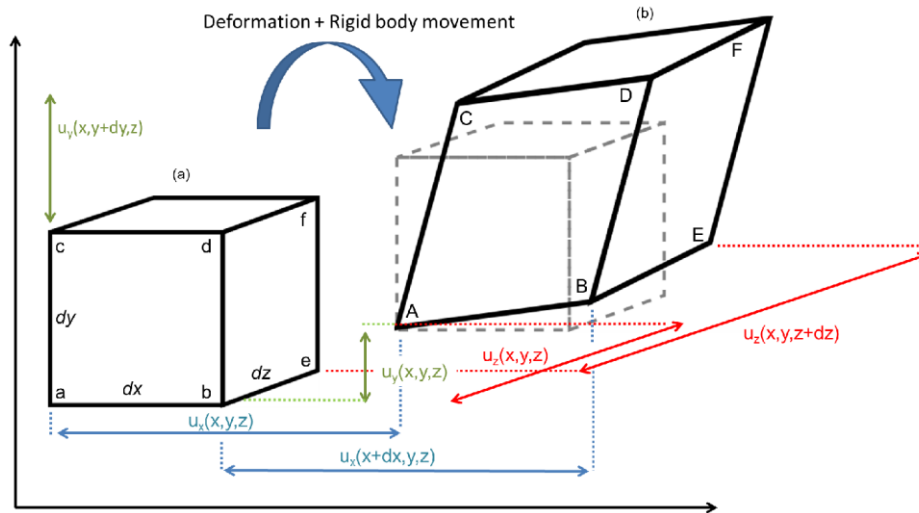


Fig 1.3: geometrical interpretation of strain [12]

And the analytic expressions are[1] :

$$\epsilon_x = \frac{\delta u_x}{\delta x} \quad (1.4)$$

$$\epsilon_y = \frac{\delta u_y}{\delta y} \quad (1.5)$$

$$\epsilon_z = \frac{\delta u_z}{\delta z} \quad (1.6)$$

$$\gamma_{xy} = 2\epsilon_{xy} = \left(\frac{\delta u_x}{\delta y} + \frac{\delta u_y}{\delta x} \right) \quad (1.7)$$

$$\gamma_{xz} = 2\epsilon_{xz} = \left(\frac{\delta u_x}{\delta z} + \frac{\delta u_z}{\delta x} \right) \quad (1.8)$$

$$\gamma_{zy} = 2\epsilon_{zy} = \left(\frac{\delta u_z}{\delta y} + \frac{\delta u_y}{\delta z} \right) \quad (1.9)$$

The state of strain can be written in matrix notation, as the state of stress[1] :

$$\begin{bmatrix} \epsilon_{xx} & \gamma_{xy} & \gamma_{xz} \\ \gamma_{yx} & \epsilon_{yy} & \gamma_{yz} \\ \gamma_{zx} & \gamma_{zy} & \epsilon_{zz} \end{bmatrix}$$

1.4 Compatibility equations and solution

The set of equilibrium equations for strain and stress state contains a lot of unknowns that makes impossible the resolution of the system. Because of this we need further information to find all the components[1].

$$\frac{\delta\sigma_x}{\delta x} + \frac{\delta\tau_{xz}}{\delta y} + \frac{\delta\tau_{xy}}{\delta z} + X = 0 \quad (1.10)$$

$$\frac{\delta\sigma_y}{\delta y} + \frac{\delta\tau_{yz}}{\delta z} + \frac{\delta\tau_{xy}}{\delta x} + Y = 0 \quad (1.11)$$

$$\frac{\delta\sigma_z}{\delta z} + \frac{\delta\tau_{xz}}{\delta x} + \frac{\delta\tau_{zy}}{\delta y} + Z = 0 \quad (1.12)$$

$$\frac{\delta^2\epsilon_x}{\delta y^2} + \frac{\delta^2\epsilon_y}{\delta x^2} = \frac{\delta^2\gamma_{xy}}{\delta x\delta y} \quad (1.13)$$

$$\frac{\delta^2\epsilon_y}{\delta z^2} + \frac{\delta^2\epsilon_z}{\delta y^2} = \frac{\delta^2\gamma_{yz}}{\delta z\delta y} \quad (1.14)$$

$$\frac{\delta^2\epsilon_x}{\delta z^2} + \frac{\delta^2\epsilon_z}{\delta x^2} = \frac{\delta^2\gamma_{xz}}{\delta x\delta z} \quad (1.15)$$

The resolution of the problem is achieved thanks to the introduction of a set of other relations that link the stress tensor and the strain tensor. All these new information are retrieved from a series of different constitutive models. A constitutive model describes the response of a material when it is stressed by an external force that could change the state of stress and the state of strain.

There are a lot of constitutive models and they describe the behaviour of a material in terms of elasticity, plasticity and viscosity.

1.4.1 Elasticity and Hooke's law

An elastic body is a type of material that returns to its original state of stress when the external applied force is retired. There is a direct relation between stress and strain. This relation could be linear or non linear.

On a cartesian plot (fig 1.4) the straight line AB represents the linear relation between stress and strain and the elastic domain[1].

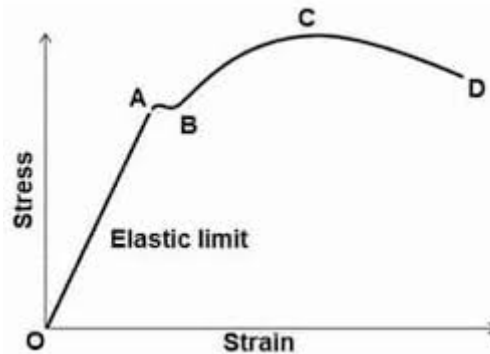


Fig 1.4: stress-strain domain and response [1]

This linear relation has been studied by Hooke that found the relation between stress and deformation (fig 1.5), deriving two different parameters directly from laboratory analysis on rock samples. The two parameters are: E (Young modulus) and ν (Poisson's ratio) [1] .

The Young modulus is a measure of the stiffness of a material and it can be retrieved from σ - ϵ as slope of it[1] .

The Poisson's ratio is a measure of the deformation of the sample due to the applied stress [1].

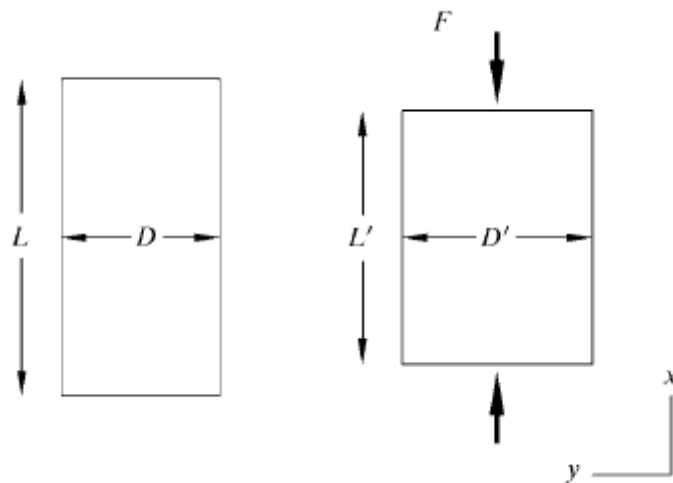


Fig 1.5: deformation induced from uniaxial stress [1]

Hooke's law[1] :

$$\varepsilon_z = \frac{L-L'}{L} \quad (1.16)$$

$$\varepsilon_z = \frac{\sigma_z}{E} \quad (1.17)$$

Where:

- L is the initial length and L' is the length after the stress application
- σ_z is the uniaxial stress applied.

$$\varepsilon_x = \varepsilon_y = \frac{D-D'}{D} \quad (1.18)$$

$$\nu = -\frac{\varepsilon_x}{\varepsilon_z} \quad (1.19)$$

Where:

- D is the initial diameter and D' is the diameter after deformation

The relation between stress and strain tensors is quite complicated because it is characterized by a set of 36 independent scalar quantities that form the elastic tensor[1]. But considering, hypothetically, that the material is isotropic and the σ - ε relation is linear, we can demonstrate that the quantities of the stiffness tensor reduce to two: E and ν . This is the simpler case of isotropic linear elastic behaviour (ILE) [1].

Thanks to these two elastic parameters we can resolve the problem of the constitutive equations and derive a set of equations useful for the characterization of the state of a sample rock.

The set of equations are below[1]:

$$\varepsilon_x = \frac{1}{E} [\sigma_x - \nu(\sigma_y + \sigma_z)] \quad (1.20)$$

$$\varepsilon_y = \frac{1}{E} [\sigma_y - \nu(\sigma_x + \sigma_z)] \quad (1.21)$$

$$\varepsilon_z = \frac{1}{E} [\sigma_z - \nu(\sigma_x + \sigma_y)] \quad (1.22)$$

$$\gamma_{xy} = \frac{2(1+\nu)}{E} \tau_{xy} \quad (1.23)$$

$$\gamma_{yz} = \frac{2(1+\nu)}{E} \tau_{yz} \quad (1.24)$$

$$\gamma_{xz} = \frac{2(1+\nu)}{E} \tau_{xz} \quad (1.25)$$

1.5 Plasticity

Plasticity refers to the behaviour of a material that is deformed after the application of a stress. The deformation in plastic domain is irreversible and leads to the failure of the material itself[1]. The onset of plastic behaviour identifies the yield point (fig 1.6).

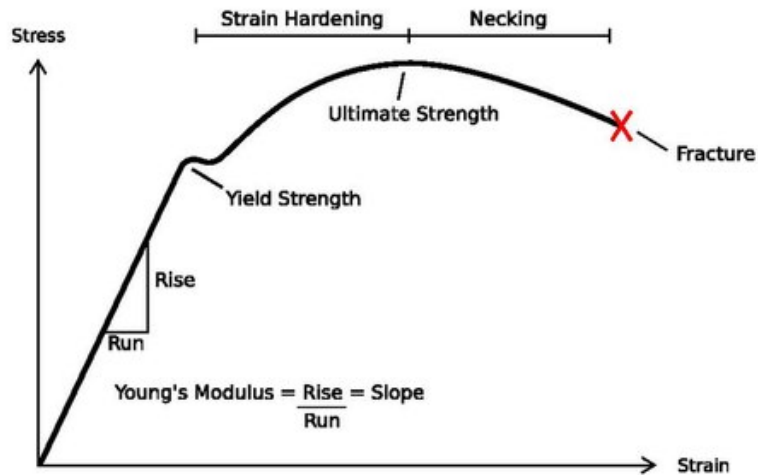


Fig 1.5: stress-strain typical curve [6]

From an analytic point of view, the total strain deformation is composed by two component (fig 1.7): ϵ^e (elastic strain increment) and ϵ^p (plastic strain increment) [1,2].

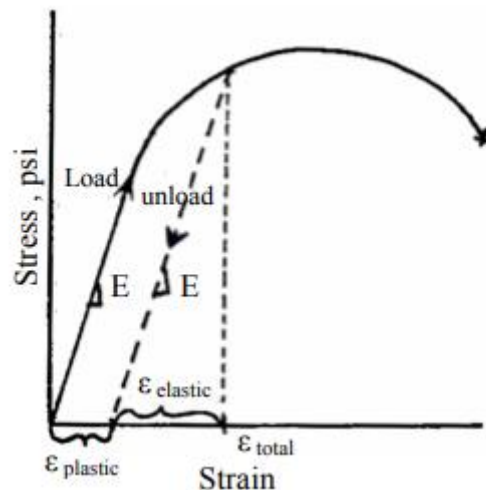


Fig 1.7: plastic deformation [2]

$$\epsilon_t = \epsilon^e + \epsilon^p \quad (1.26)$$

1.6 Essentials of strength criteria

The strength of a rock is the maximum stress that a material can bear, after which the rock fails and fracture occurs. In geomechanics is also called *ultimate strength* or *peak strength* (fig 1.5) [1]. A fracture occurs when planes of deformations start to form in the rock. The rock starts to fail when the material, under stress, reaches the ultimate strength; after this point the rock has a minimum strength called *residual strength*[1].

The failure of a rock sample occurs when a specific state of stress is reached. The level of stress that leads to the failure can be evaluated considering different failure criteria, empirical or not, studied by scientists (Tresca, Mohr, Coulomb, Griffith).

1.6.1 Mohr-Coulomb criterion

Mohr-Coulomb criterion is the most used failure criterion used in geomechanics analysis. It is based on the study of the state of stress of rock bodies. Mohr and Coulomb understood that the *failure of a sample occurs when the Mohr's circle (state of stress) touches a failure envelope*[1].

Considering a rock sample stressed by a uniaxial and a confining stress (fig 1.8) , during a lab test:

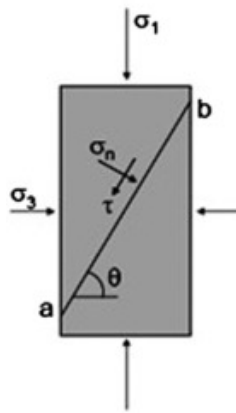


Fig 1.8: rock sample stressed [1]

The failure envelope is a graphical representation of the relationship[1]:

$$\tau_s = S_0 + c' \tan \theta \quad (\text{Eq. 1.27})$$

Where S_0 represents the cohesion of the material which is the critical level of shear stress at which the material yields (Mohr Hypothesis) and θ is the internal friction angle [1].

Graphically:

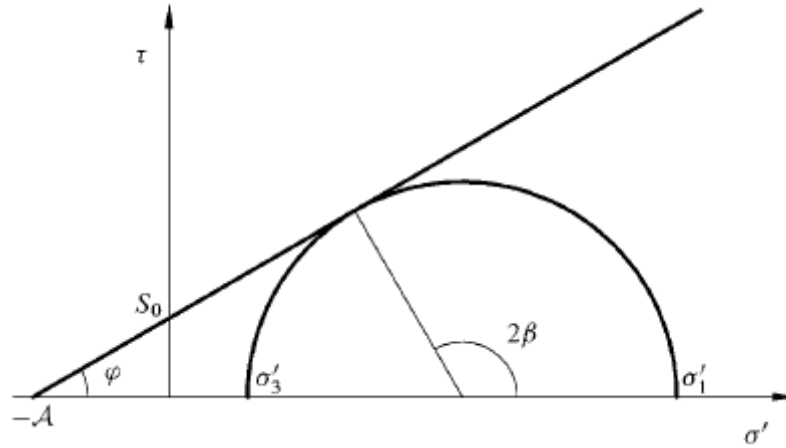


Fig 1.9: Mohr-Coulomb criterion[1]

It can be seen from the plot that 2β is the angle at which the Mohr circle touches the failure line, and consequently it is the angle of the plane where the fracture forms and the sample fails [1].

The shear stress at which this occurs is:

$$\tau = \frac{1}{2}(\sigma'_1 - \sigma'_3) \sin 2\beta \quad (\text{Eq. 1.28})$$

And the corresponding normal stress is:

$$\sigma' = \frac{1}{2}(\sigma'_1 + \sigma'_3) + \frac{1}{2}(\sigma'_1 - \sigma'_3) \cos 2\beta \quad (\text{Eq. 1.29})$$

And $\theta + \frac{\pi}{2} = 2\beta$.

Combining Eq.1.27, Eq.1.28 and Eq.1.29, we obtain[1]:

$$\sigma'_1 = 2S_0 \frac{\cos \theta}{1 - \sin \theta} + \sigma'_3 \frac{1 + \sin \theta}{1 - \sin \theta} \quad (\text{Eq. 1.30})$$

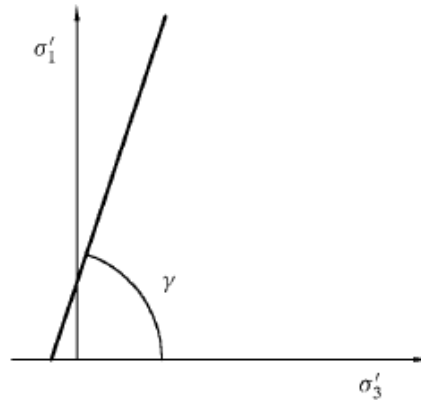


Fig 1.10: Mohr-Coulomb criterion in effective stress domain[1]

This different way to write the Mohr-Coulomb criterion helps us to identify other two strength parameters: uniaxial compressive strength (UCS or C_0) and tensile strength (T_0) [1].

$$\text{When we take } \sigma'_3 = 0 \text{ we obtain } UCS = 2S_0 \frac{\cos \theta}{1 - \sin \theta} \quad (1.31)$$

$$\text{When we take } \sigma'_1 = 0 \text{ we obtain } T_0 = \frac{2S_0 \cos \theta}{1 + \sin \theta} \quad (1.32).$$

1.6.2 Hoek & Brown empirical criterion

Hoek & Brown criterion was introduced to study stability during excavation. It is an empirical criterion deriving from triaxial lab tests carried out on rock samples in the 80's.

The main target of this criterion is that the slope of the failure envelope decreases as the confining pressure increases. It is no more a linear relation but a power law (fig 1.11) [1,3,4]:

$$\sigma'_1 = \sigma'_3 + (mC_0\sigma'_3 + sC_0^2)^{0.5} \quad (1.33)$$

Where:

- m and s are dimensionless strength parameters;
- m is derived from lab tests;
- m varies with rock type;
- s depends on rock characteristics.

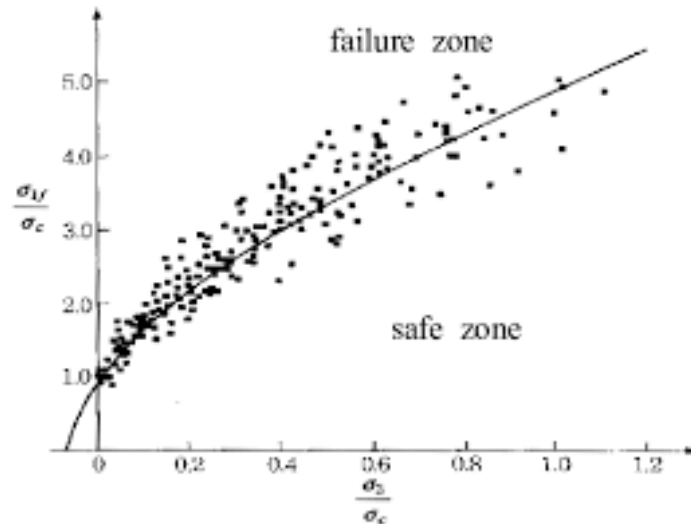


Fig 1.11: Empirical Hoek & Brown criterion plot [3]

1.6.3 Griffith model

Griffith studied the phenomena of crack formation and development inside a rock. He postulated that “*fracture of brittle materials is initiated at tensile stress concentrations at the tips of minute thin cracks, distributed throughout an isotropic elastic material. When the tensile stress at a tip of a material will exceed the natural tensile strength of the material, the crack initiates and propagates*” [1].

The model is written in terms of tensile strength[1] :

$$(\sigma_1 - \sigma_3)^2 = 8T_0(\sigma'_1 + \sigma'_3) \quad \text{if} \quad (\sigma'_1 + 3\sigma'_3) > 0 \quad (1.34)$$

$$\sigma'_3 = -T_0 \quad \text{if} \quad (\sigma'_1 + 3\sigma'_3) < 0 \quad (1.35)$$

In the principal stress plot the model is represented by a parabola (fig 1.12):

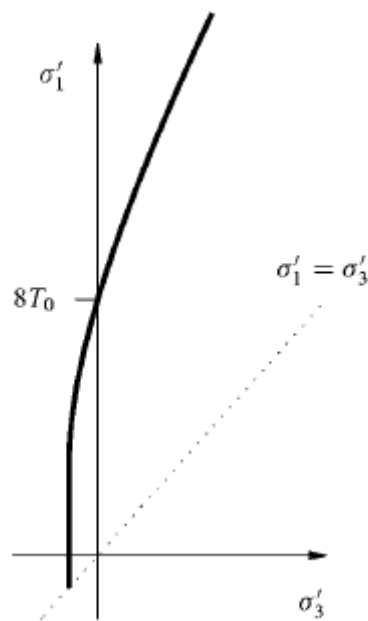


Fig 1.12: Griffith criterion[1]

The intercept identifies the uniaxial compressive strength UCS (confining pressure is null).

1.7 Anisotropy rocks

The assumptions made to describe the geomechanics theory are based on the fact that the rock is considered isotropic (properties don't change along the different directions). In nature, the situation is more complex and the isotropy is not more valid.

There are different types of anisotropy[1]:

- Transverse isotropy when there are plane of symmetry parallel along which the properties of the material are no more constant;
- Orthorhombic isotropy when there are three perpendicular plane of symmetry.

The presence of plane of symmetry along which the properties are no more constant makes an important role in the stability of the rock and lead to complex problems during excavation and drilling.

1.7.1 Plane of weakness model

The plane of weakness model is the easiest way to understand the failure of anisotropic rocks.

This model concerns the stability of materials that have assumed the strength is the same along all the directions except for one set of parallel planes along which the strength is lower.

The inclination of the weakness planes is important during stability analysis and may have an effect on it.

The plane of weakness model correlates this inclination to the applied stresses and other failure criteria.

Considering a sample rock with bedding inclination indicated with β_w (fig 1.13) [1]:

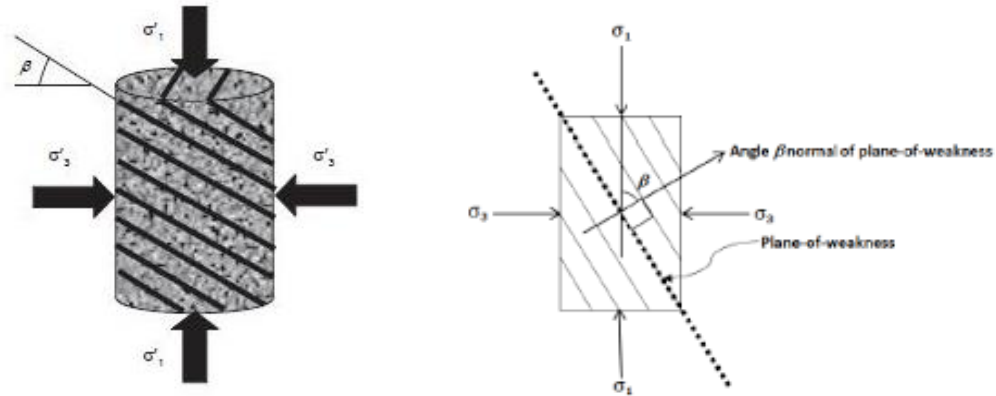


Fig 1.13: sample rock with transverse isotropy[1]

A first consideration that we can do is: the lower strength of weakness planes makes the sample failure easier (the applied load should be lower then in the case of pure isotropic material) [1,5].

For this reason, the envelope failure on Mohr-Coulomb plot could be smaller too.

In fact, on the plot we will find two failure envelopes; the intrinsic envelope characteristic of the isotropic material, and the weak plane envelope characteristic of transverse isotropic material (fig 1.14) [1].

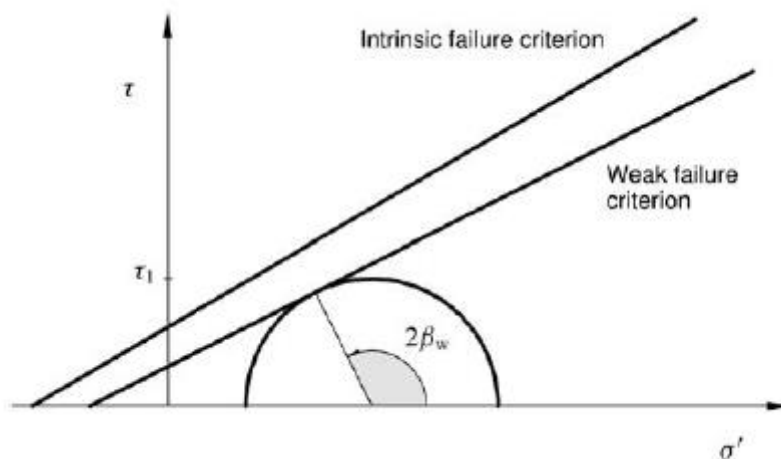


Fig1.14 : plane of weakness model[1]

As in the case of Mohr-Coulomb criterion, we will have a set of equations that concerns the problem[1]:

$$\tau = \frac{1}{2}(\sigma'_1 - \sigma'_3) \sin 2\beta_w \quad (1.36)$$

$$\sigma' = \frac{1}{2}(\sigma'_1 + \sigma'_3) + \frac{1}{2}(\sigma'_1 - \sigma'_3) \cos 2\beta_w \quad (1.37)$$

That, combined with the MC criterion $\tau_s = S_{o,w} + c' \tan \theta_w$ (1.38) gives us the amount of applied stress at which the slip along the joint starts [1] :

$$(\sigma_1 - \sigma_3)_{slip} = \frac{2(S_{o,w} + \sigma'_3 \tan \theta'_w)}{((1 - \tan \theta'_w \cot \beta_w) \sin 2\beta_w)} \quad (1.39)$$

The minimum strength occurs when $\beta_w = 45^\circ + \frac{\theta'_w}{2}$ (fig 1.15):

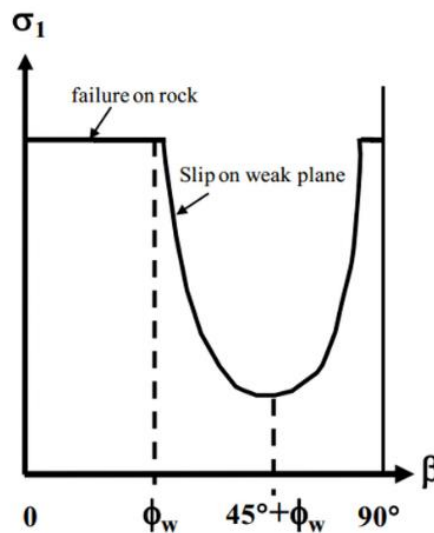


Fig 1.15: minimum strength plot [8]

1.8 Terzaghi Principle

In soil and rock mechanics the presence of water makes an important state relative to the state of stress and relative change. All the phenomena related to rock mechanics (deformation, compaction, subsidence, etc) depend on effective stress and not on total stress[1].

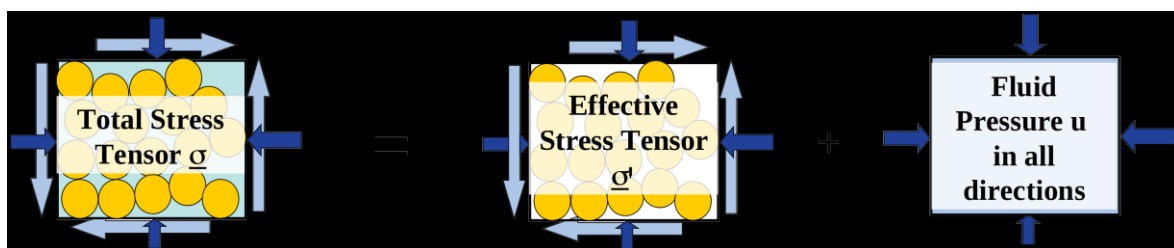


Fig 1.16 : representation of Terzaghi's principle [9]

The effective stress is:

$$\sigma'_{ij} = \sigma_{ij} - u\alpha\delta_{ij} \quad (1.40)$$

Where:

- σ'_{ij} is the effective stress tensor;
- σ_{ij} is the total stress tensor;
- u is the pore pressure;
- α is the Biot's coefficient (is equal to 1 for soils, 0 for rock);
- δ_{ij} is the Kroneker delta.

This principle is useful to calculate geostatic stresses relative to a certain depth in the subsoil, for vertical and horizontal direction[1].

2. STRESS AROUND BOREHOLE

In underground formations the state of stress depends mostly on overburden and on geological history the rock has been subjected during the eras.

During excavation or drilling process, the state of stress can undergo changes especially when rock material is removed.

2.1 Cylindrical coordinates

To better explain the situation the boreholes are subjected, we need to analyse the model considering cylindrical coordinates.

Schematically, the borehole model can be represented as in fig 2.1:

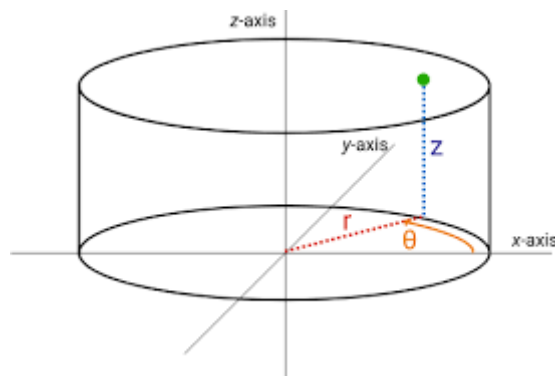


Fig 2.1: schematic representation of a borehole and cylindrical coordinates [7]

Where z represents the axial direction, r the radial direction and θ the tangential direction.

2.2 Stresses and strains

Considering an engineering point of view the stress and strains of a point P in the rock can be mathematically expressed in 3D (fig 2.2) as a stress tensor [1] :

$$\begin{bmatrix} \sigma_{rr} & \tau_{r\theta} & \tau_{rz} \\ \tau_{\theta r} & \sigma_{\theta\theta} & \tau_{\theta z} \\ \tau_{zr} & \tau_{z\theta} & \sigma_{zz} \end{bmatrix}$$

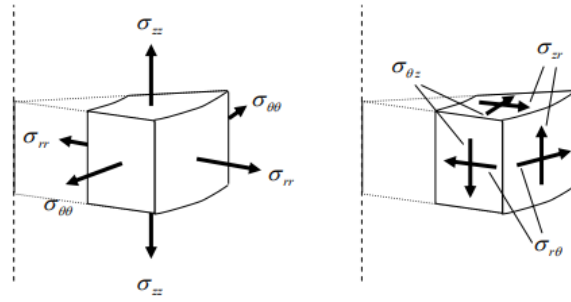


Fig 2.2 : 3D model of stress tensor in cylindrical coordinates[1]

In borehole stability analysis the situation is simplified by the fact that we consider a 2D model (the stress in a plane perpendicular to the axis of excavation) (fig2.3):

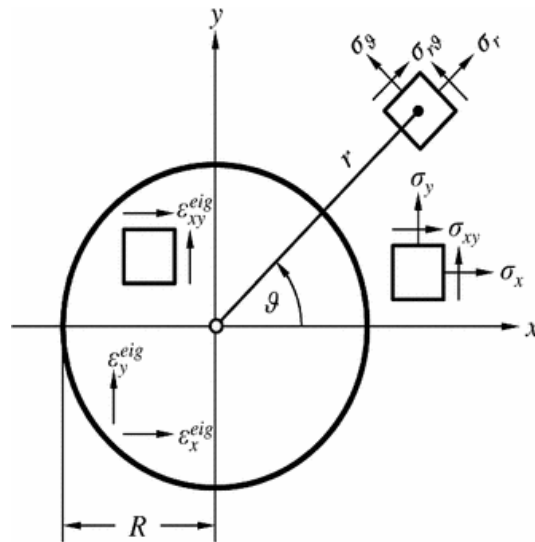


Fig 2.3: stress state in 2D [10]

And the corresponding tensor is[1]:

$$\begin{bmatrix} \sigma_{rr} & \tau_{r\theta} \\ \tau_{\theta r} & \sigma_{\theta\theta} \end{bmatrix}$$

Where:

$$\sigma_r = \frac{1}{2}(\sigma_x + \sigma_y) + \frac{1}{2}(\sigma_x - \sigma_y) \cos 2\theta + \tau_{xy} \sin 2\theta \quad (2.2)$$

$$\sigma_\theta = \frac{1}{2}(\sigma_x + \sigma_y) - \frac{1}{2}(\sigma_x - \sigma_y) \cos 2\theta - \tau_{xy} \sin 2\theta \quad (2.3)$$

$$\sigma_z = \sigma_z \quad (2.4)$$

$$\tau_{r\theta} = \frac{1}{2}(\sigma_y - \sigma_x) \sin 2\theta + \tau_{xy} \cos 2\theta \quad (2.5)$$

$$\tau_{rz} = \tau_{xz} \cos 2\theta + \tau_{yz} \sin 2\theta \quad (2.6)$$

$$\tau_{\theta z} = \tau_{yz} \cos 2\theta - \tau_{xz} \sin 2\theta \quad (2.7)$$

2.3 Hints about State of stress for anisotropic conditions

The model of infinite hollow cylinder has been assumed to describe the geomechanics characterization of the rocks during excavations and the corresponding problems which derive from the possible failure of the rock[1].

The borehole is a full rotational symmetry around the principal axis (z) which is subjected to overburden stress σ_v and far field stresses perpendicular to the wall of the borehole. The far field stresses can develop isotropically (the stress is equal from every direction) or anisotropically (different stresses from different directions) [1] (fig2.4).

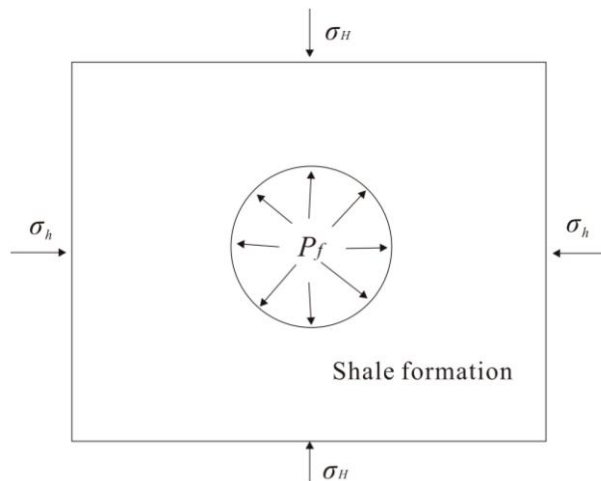


Fig 2.4 : Anisotropic far field formation state of stress [1]

The problem of anisotropic far field stress state has been studied and explained by Kirsch that gave us a general solution for vertical borehole in terms of total stresses[1]:

$$\sigma_r = \frac{1}{2}(\sigma_h + \sigma_H) \left(1 - \frac{R_w^2}{r^2}\right) + \frac{1}{2}(\sigma_H - \sigma_h) \left(1 + \frac{3R_w^4}{r^4} - \frac{4R_w^2}{r^2}\right) \cos 2\theta + p_w \frac{R_w^2}{r^2} \quad (2.8)$$

$$\sigma_\theta = \frac{1}{2}(\sigma_h + \sigma_H) \left(1 + \frac{R_w^2}{r^2}\right) - \frac{1}{2}(\sigma_H - \sigma_h) \left(1 + \frac{3R_w^4}{r^4}\right) \cos 2\theta - p_w \frac{R_w^2}{r^2} \quad (2.9)$$

$$\sigma_z = \sigma_v - 2\nu(\sigma_H - \sigma_h) \left(\frac{R_w^2}{r^2}\right) \cos 2\theta \quad (2.10)$$

$$\tau_{r\theta} = -\frac{1}{2}(\sigma_H - \sigma_h) \left(1 - \frac{R_w^2}{r^2}\right) \left(1 - \frac{3R_w^4}{r^4} + \frac{4R_w^2}{r^2}\right) \sin 2\theta \quad (2.11)$$

$$\tau_{\theta z} = \tau_{rz} = 0 \quad (2.12)$$

Which at borehole wall (when $r = R_w$) become:

$$\sigma_r = p_w \quad (2.13)$$

$$\sigma_\theta = \sigma_H + \sigma_h - 2(\sigma_H - \sigma_h) \cos 2\theta - p_w \quad (2.14)$$

$$\sigma_z = \sigma_v - 2\nu_{fr}(\sigma_H - \sigma_h) \cos 2\theta \quad (2.15)$$

$$\tau_{r\theta} = \tau_{\theta z} = \tau_{rz} = 0 \quad (2.16)$$

Because of the anisotropy of the stresses, it is possible to see that along the borehole the effect of the far field stresses is different (fig 2.5); the mean stress p is not uniform and lead to different effect in the hole[1]:

$$\sigma_r + \sigma_\theta + \sigma_z = \sigma_v + \sigma_h + \sigma_H - 2(1 + \nu)(\sigma_H - \sigma_h) \frac{R_w^2}{r^2} \cos 2\theta \quad (2.17)$$

$$p = \frac{1}{3}(\sigma_r + \sigma_\theta + \sigma_z) \quad (2.18)$$

Eq. 2.16 and 2.17 show how the far field anisotropy effects the mean stress and consequently the volumetric changes of the borehole and the possible failures that can occur [1].

When $\theta=0^\circ$ $\sigma_r + \sigma_\theta + \sigma_z = \sigma_v + \sigma_h + \sigma_H - 2(1 + \nu)(\sigma_H - \sigma_h)$ and the mean stress decreases.

When $\theta=90^\circ$ $\sigma_r + \sigma_\theta + \sigma_z = \sigma_v + \sigma_h + \sigma_H$ and the mean stress increases.

In the direction of the maximum field stress could be instability problems due to the volumetric changes of the rock, breakout can occur.

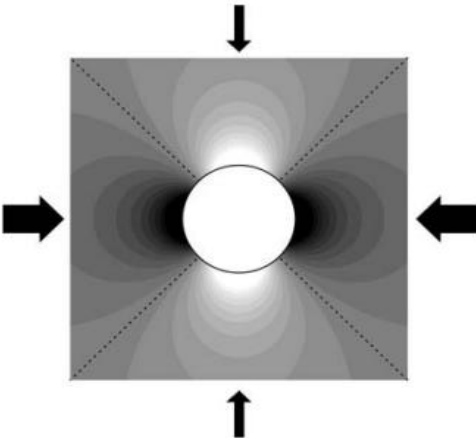


Fig 2.5: changes in mean stress, the black indicates a decrease in mean stress while white an increase in mean stress[1]

3. Modelling of Wellbore stability in transversely isotropic formation

The earth's crust is characterized by several different complex formations whose geomechanics properties cannot be considered constant in all the directions. During drilling operations, a lot of problems related to rock anisotropy are involved in the planning process to avoid failure of the borehole.

The geological history of a formation is depending upon all the natural transformations that the rock can undergo during the time. Diagenesis, tectonic movements, sedimentation and erosion play an important role: the bedded formation's feature is the presence of weakness planes which have different properties with respect the entire rock [13,14].

It is said that a transversely isotropic material has properties symmetric along an axis that is normal to the isotropic plane (fig3.1) [15].

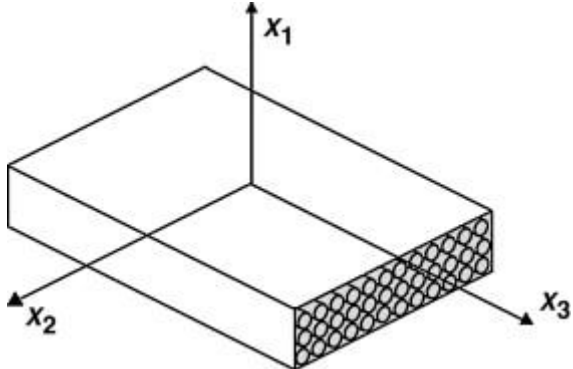


Fig 3.1: schematization of transversely isotropic material[16]

The main role involved in the stability analysis of this type of formation is the inclination of the bedding planes (fig 3.2) [16].

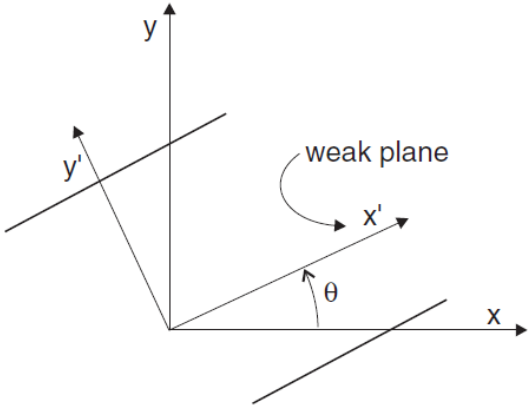


Fig 3.2: inclination of bedding planes [16]

The critical situation is when the anisotropy plane is sub-parallel to the axis of the wellbore; in horizontally bedded formation no stability problems, related to drilling process, have been encountered yet.

The modelling is conducted to evaluate the stability of this sub-parallel weakness plane and the influence that they have on vertical wellbore (fig 3.3) [17].

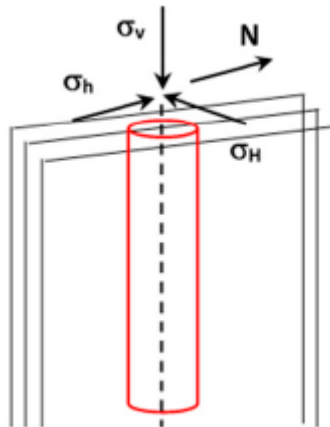


Fig 3.3: scheme of a well drilled in vertically bedded formation and indication of far fields stresses[17].

3.1 Fast Lagrangian analysis of Continua (FLAC) implementation

FLAC is numerical modelling software for complex analysis of soil, rock, groundwater, and ground support in geotechnical engineering field. It is designed to deal with any kind of geotechnical engineering problem that requires continuum analysis.

The first step to follow in the *FLAC* modelling is to create a structure in two dimension that can represent our model; i have created, according to all the functions present in the software, a hole section representing a wellbore in a stressed field (fig3.4).

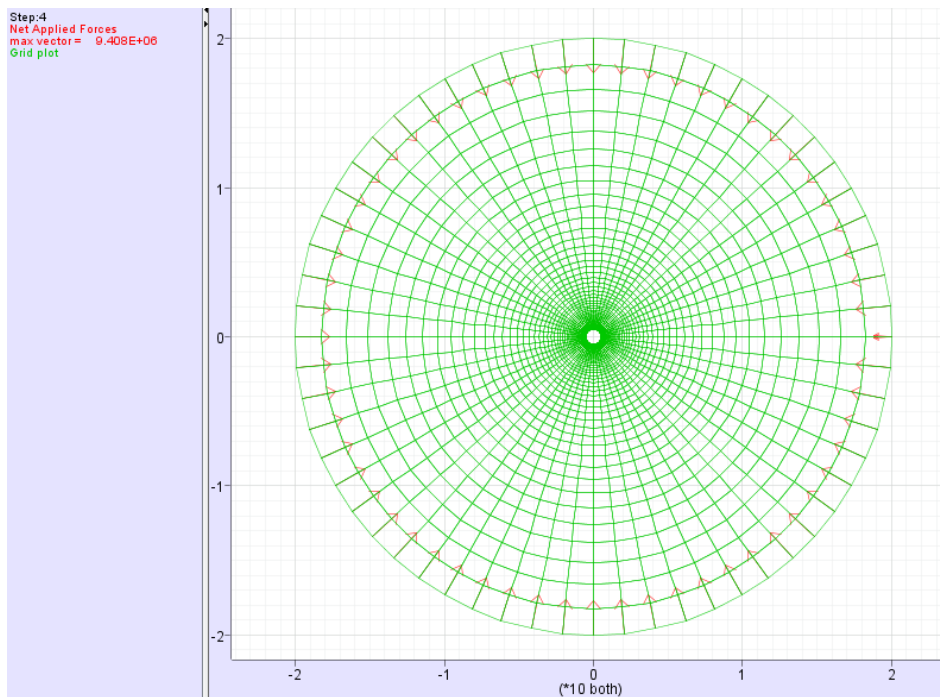


Fig 3.4: wellbore modelling in FLAC with far field stress application with red arrows (obtained from FLAC)

Once, we have created this model, we can implement by writing the code the constitutive model we have chosen to analyse the slip along the joint.

In particular, on FLAC, two methodologies can be used to do this[16]:

1. Ubiquitous-joint model for undrained conditions;
2. Ubiquitous-joint model for drained conditions.

Obviously, each of the named model need different input data and because of this, they will give different results which should be consistent each other.

3.2 Formation parameters

Different kind of traps involve the hydrocarbon accumulation in the subsurface. The main structures that define them are: a bearing-hydrocarbon zone (with high porosity and high permeability) and a cap-rock (low porosity and low permeability). For drilling related problems the main role is played by cap rock, generally shale or clay, which must be drilled to reach hydrocarbon bearing zone, and must be maintained stable and intact to not make the formation weak and lead to a failure that can cause slip and problem on drilling string and casing. These kind of formations, today are also considered unconventional gas and oil reservoirs because can trap (in low quantity with respect to high-porous media) hydrocarbons such as oil-shale or gas-shale that require innovative extraction process or accurate classical drilling process. A different use of these not-permeable formations is to trap nuclear waste.

For all the above reasons, different shale formations have been studied during the last decades: posedonia shale (Germany) and opalinus clay (Switzerland).

3.2.1 Posedonia shale

The Posidonia Shale is a very distinctive formation placed in north western Europe, distributing from the United Kingdom to Germany [18]. The formation of posedonia shale is around 30–60 m of dark-grey to brownish-black, bituminous, fissile claystone sand. It is commonly suggested that the Posidonia Shale was probably deposited over a large area during a period of high sea level and restricted seafloor circulation. The Posidonia Shale Formation developed conformably on the nonbituminous claystones of the Lower Jurassic Aalburg Formation [19,20]. The formation consists of dark-gray to brownish-black bituminous fissile claystones.

A lot of studies have been conducted on Posedonia shale; the most of the work has been done by Meier (2013) and others which investigated for physical and chemical properties of this kind of formation [21, 22, 23, 24].

TABLE 3.1: PARAMETERS MEASURED BY MEIER [21,24]

MATURITY	0.88
POROSITY	1.1±0.3
CALCITE CONTENT	47.3±0.5 %
CLAY CONTENT	27.8±1.6 %
QUARTZ CONTENT	17.2±0.4 %
PYRITE	5.3±0.2 %
TOC	5.8 ± 0.3 %
WATER CONTENT	1 %

And the geomechanics properties are the following:

TABELLA 3.2: GEOMECHANICS PRAMETERS, WITH A THOSE MEASURED BY MEIER AT 2013 AND 2017 [21, 23]

E_{XY}^A	17.3 GPa
G_{XY}	8.9 GPa
UCS_{XY}	75 ± 7 MPa
UCS_{45}	60 ± 10 MPa
UCS_Z	115 ± 7 Mpa
G_Z	5.5 GPa
E_Z^A	10.4 GPa
E_{XY}/E_Z	1.66
POISSON RATIO ν_{XY}	0.18
POISSON RATIO ν_{YZ}	0.17
K	10^{-22} m^2
FRICION ANGLE	20°
C	20 MPa

3.2.2 Opalinus clay

The Mont Terri Rock Laboratory [25], located in North West Switzerland in an argillaceous formation known as the Opalinus Clay, has been the site of geotechnical research since 1995. The focalization is due to the fact that opalinus clay can be used to contain and treat radioactive waste because of the natural isolation power of it. A lot of lab experiments have been done to best characterize the geomechanical and seismic properties of this type of rock. The definition of clay to the opalinus formation, which is a shale rock, is deriving from the high content of clay, around 60% [25] and it is defines as clay-shale formation. The study on this type of formation help us, also, to study the behaviour of similar formations, like unconventional gas shale formations [26].

Opalinus Clay (fig 3.5) is composed of 50–65% of clay, and mineralogy consisting of kaolinite and illite [29].

From the point of view of petrophysics, the main properties have been measured by different scientists [27,28,29,30] summarized in the following tables:

TABLE 3.3: PETROPHYSICS PARAMETERS MEASURED BY BOCK (IN 2001) AND WILLNEAUV (IN 2005) [27]

BULK DENSITY ^B	2450 ± 30 kg m ⁻³
DRY BULK DENSITY ^B	2340 ± 60 kg m ⁻³
GRAIN DENSITY ^B	2710 ± 30 kg m ⁻³
ELASTIC BULK MODULUS ^B	8.7 GPa
WATER CONTENT ^B	6.1 ± 1.9 %
POROSITY ^B	13.7 ± 3.1 %
CLAY CONTENT ^W	62 %
CARBONATE CONTENT ^W	14 %
QUARTZ CONTENT ^W	18 %

According the different loading history that a material has undergone during the time, the rock can be considered not isotropy. All the characteristic parameters, deriving from different lab tests, could vary.

A lot pf tests have been performed and in the followed table (table 3.4) we have a summary of the most important, conducted by Bock, Willenauv and Gens [27]:

TABLE 3.4: GEOMECHANICS PARAMETERS MEASURED IN LAB BY BOCK IN 2001 (INDICATED WITH W), BY WILLEVEAU IN 2005 (INDICATED BY W) AND BY GENS IN 2007 (INDICATED BY G); NOT ALL THE PARAMETERS HAVE BEEN MEASURED DURING THE DIFFERENT TESTS [27]

TANGENT MODULUS E_T	Perpendicular	3000 ^B MPa	
	Parallel	4000 ^B Mpa	
YOUNG'S MODULUS E	Perpendicular	4000 ^B MPa	5800 ^G MPa
	Parallel	10000 ^B MPa	9300 ^G MPa
POISSON'S RATIO ν	axial	0.33 ^B	
	radial	0.24 ^B	0.295 ^G
SHEAR MODULUS G	-	4400 ^B MPa	
UCS	Perpendicular	16 ^B MPa	
	Parallel	10 ^B MPa	
UTS	Perpendicular	1 ^B MPa	0.5 ^W MPa
	Parallel	2 ^B MPa	1 ^W MPa
SHEAR STRENGTH C'	Perpendicular	5 ^B MPa	
	Parallel	2.2 ^B MPa	
FRICTION ANGLE OF MATERIAL Φ'	-	25 ° ^B	
SHEAR STRENGTH OF BEDDING PLANES C'_{BEDDING}	-	1 ^B MPa	
FRICTION ANGLE OF BEDDING PLANES Φ'_{BEDDING}	-	23 ° ^B	

A series of experimental tests have carried out on opalinus clay samples to understand the geomechanical behaviour and to predict the conditions at the sample fails.

In general, the mechanical behaviour of the opalinus clays is mostly subjected by the presence of planes of anisotropy. The most of the tests showed a brittle mechanical behaviour and different paths of break due to the inclination of the planes, in the different samples [31,32,33]



Fig 3.5: opalinus-clay formation [34]

3.3 FLAC METHODOLOGY

In this section is explained how the parameters have been implemented in the code FLAC. For the modelling of the wellbore had been used the Flac Fish function of a shaped donut that includes a drilled hole surrounded by a large anisotropic stressed far field[16].

In the horizontal direction of the hole (x-direction) we can find the σ_{max} (7 MPa) while in the vertical direction (y-direction) we can find the σ_{min} (5 MPa) and the overburden component of stress, σ_z , is about 6 MPa.

The rock geomechanics characteristics used, for the opalinus clay, are summarized in table 3.4 and implemented in a ubiquitous-joint-model which accounts for the Mohr-Coulomb failure criteria[16].

The ubiquitous-joint-model is used to analyse the stability of formation (wellbore, rock block, slopes) that affected by the presence of weakness plane (set parallel) along which the properties make the formation weaker; yielding can occur along joints (slipping) or in the solid rock (breaking) [16,35] .

The stresses are resolved locally using the set of equations below[16]:

$$\sigma'_{11} = \sigma_{11} \cos^2 \theta + 2\sigma_{12} \sin \theta \cos \theta + \sigma_{22} \sin^2 \theta \quad (3.1)$$

$$\sigma'_{22} = \sigma_{11} \sin^2 \theta - 2\sigma_{12} \sin \theta \cos \theta + \sigma_{22} \cos^2 \theta \quad (3.2)$$

$$\sigma'_{33} = \sigma_{33} \quad (3.3)$$

$$\sigma'_{12} = -(\sigma_{11} - \sigma_{22}) \sin \theta \cos \theta + \sigma_{12}(\cos^2 \theta - \sin^2 \theta) \quad (3.4)$$

the global failure criterion account for $f_s=0$ and $f^t=0$, considering Mohr-Coulomb law (fig 3.5) [16]:

$$f_s = -\tau - \sigma'_{22} \tan \phi_j + c_j \quad (3.5)$$

$$f^t = \sigma_j^t - \sigma'_{22} \quad (3.6)$$

where:

- ϕ_j is the friction angle;
- c_j is the cohesion of the formation;
- σ_j^t is the tensile strength of weakness planes;
- $\tau = |\sigma'_{12}|$.

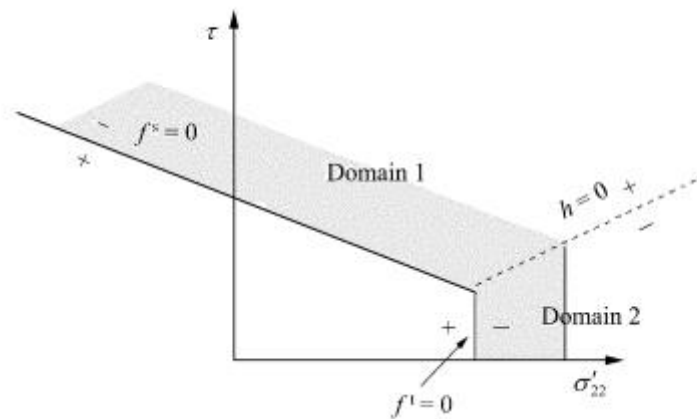


Fig 3.5: ubiquitous-joint model criterion; the function $h(\sigma'_{12}, \tau)=0$ represents the diagonal between domain 1 and domain 2 [16,36].

The failure states either in domain 1 and domain 2. If the stress state falls into domain 1 shear failure takes place in the weakness plane, while if the stress state is placed in the domain 2 the failure, tensile, is taken for sure in the entire block considered [36].

The code Flac follows the procedure to assure where the induced failure (if any) by far field stress is and sometimes considering plastic correction, because of mathematical issues of the analysis.

The study has been conducted considering different bedding planes orientation, δ , from 0° to 170° (fig 3.7) [17,33]:

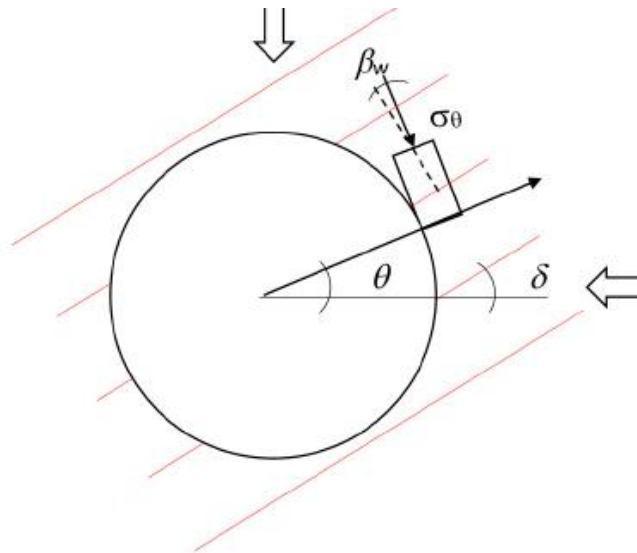


Fig 3.6: wellbore in a bedded formation, δ is the bedding inclination [17]

I started with the case of saturated formation (pore pressure of 2.5 MPa) and the hole filled with fluid (fluid pressure of 2.6 MPa) able to bear the walls of the wellbore (fig 3.7).

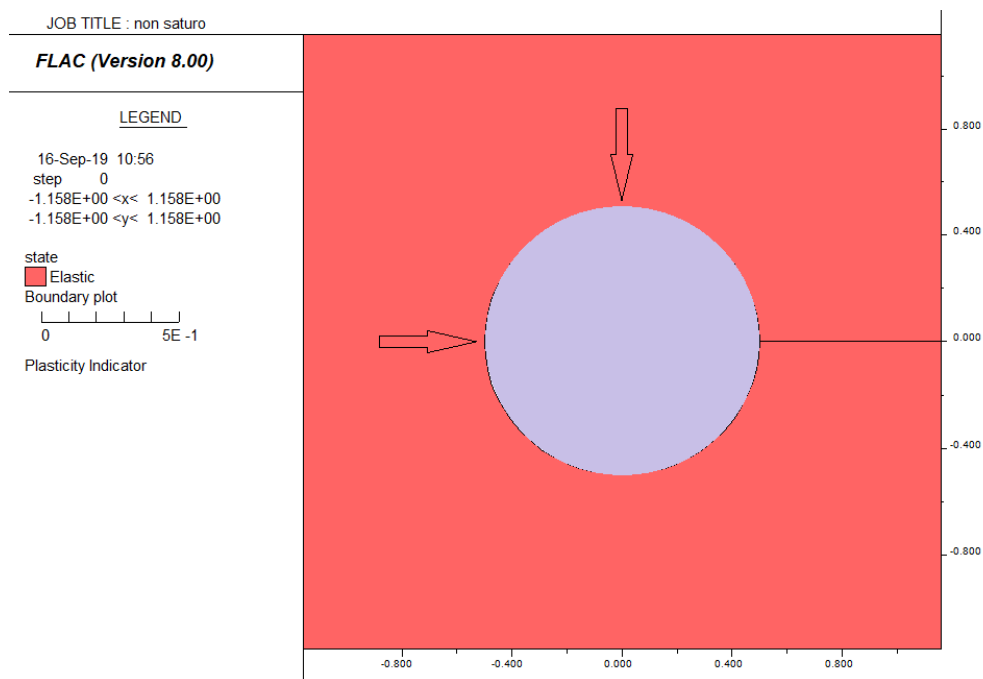


Fig 3.7: FLAC model showing a wellbore drilled in an anisotropic stress far filed filled with fluids that sustain wellbore walls, no failure detected (from FLAC).

The main aim of this study is to evaluate the influence of the bedding planes inclination in the stability of a wellbore, and, in case, to forecast where the slip along the joints will occur.

On the two formations, the modelling has been conducted by considering two different cases:

1. Undrained condition (the situation in which a rock element does not exchange water. In conditions of total saturation, the volume variations are null) (APPENDIX A);
2. Drained condition (the condition in which, for each point of rock, the variation of the effective stresses is equal to the variation of the total tensions. A water flow is simulated during a time interval) (APPENDIX B).

The undrained condition simulation does not consider a water flow from the pore volume to the external space, so the consolidation time used in the code is null. While, for drained conditions, the consolidation time used as reference is about 50000 seconds, that means 15 days. The choose of this characteristic time interval refers to a the fact that a wellbore does not stay unfilled for a long period because of the failure and collapse.

In the next chapter all the results deriving from the simulations (opalinus clay with ubiquitous-joint model in drained and undrained conditions) are summarized, and the angle of slipping is indicated.

For the posedonia shale, I also investigated the behaviour in an isotropic far field stress to compare the result obtained by Meier in 2004, on dry sample.

4. SIMULATION RESULTS

FLAC simulations have produced a lot of charts showing, depending on bedding planes inclination δ , different results.

In the following chapter, all the results will be showed and analysed trying to interpret and to decide which kind of drilling fluids to use in the drilling process, in order to sustain the wellbore walls.

The interpretation of the results is organised in two section: one for the undrained simulation, the other for drained simulation.

4.1 Opalinus Clay failure simulation

4.1.1 Undrained conditions process simulation

The undrained conditions process considers that the pore water of the formation does not move. The formation is fully saturated but no changes in volume are allowed.

Different inclinations (δ) of weakness planes have been implemented, from 0° to 170° (counter-clockwise), and the results from FLAC show how the formation, near the wellbore wall, fails and in which direction the slip of ubiquitous joint occurs.

Below all the simulation's results obtained:

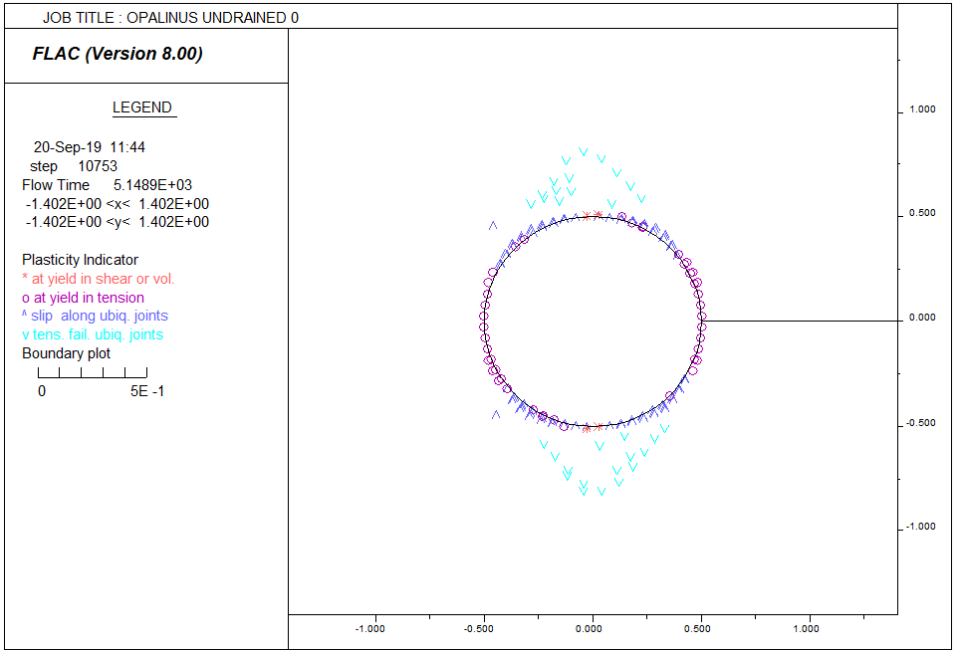


Fig 4.1 : plasticity state after consolidation of the with bedding planes inclined of 0° (obtained from FLAC analysis)

In Fig4.1 is showed the plasticity state of the formation, when the inclination of the bedding planes is of 0°. Here we can see, more clearly, where the formation breaks and the slip along the joint occurs. The blue arrows show the zone near the wellbore where the slipping occurs. Imagine to analyse the upper semicircle; we can see that the slipping along the joints develops from, around, 45° to 135° and concentrate near the wellbore wall.

The turquoise arrows show, for the ubiquitous joints, where the formation undergoes tensile failure, in the direction of the maximum far field stress (applied along the y-direction).

The violet circles show where the formation is in tension at yield point, after which plastic deformation starts.

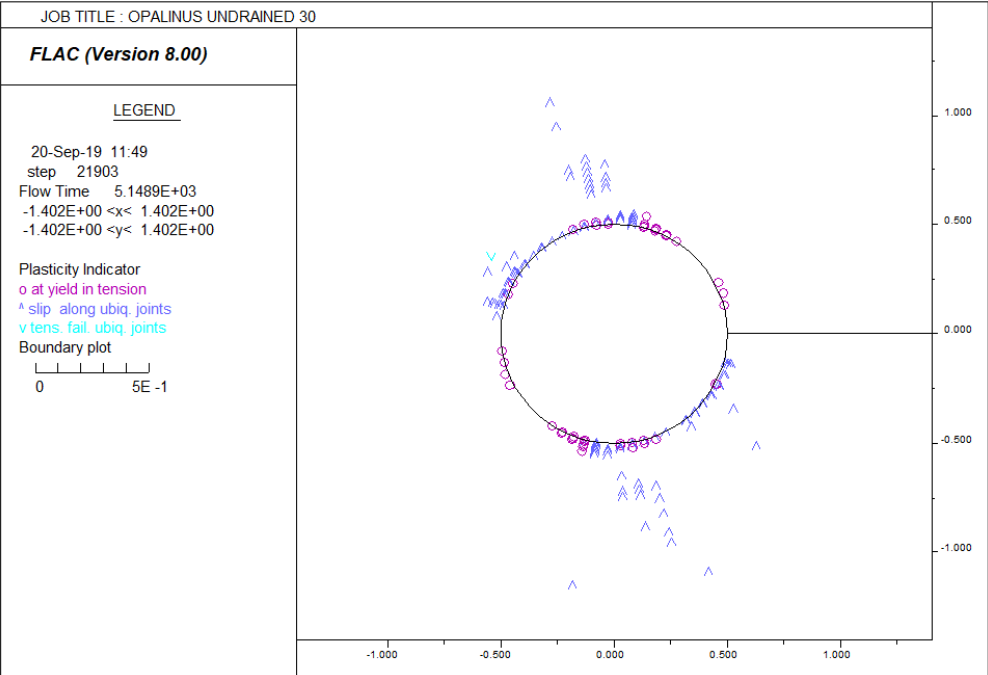


Fig 4.2: plasticity state after consolidation of the with bedding planes inclined of 30° (obtained from FLAC analysis)

In Fig4.2 is showed the plasticity state of the formation, when the inclination of the bedding planes is of 30°.

The slip along ubiquitous joints, in this case, is concentrated in arc of the wellbore from 80° to 170° and far from the wellbore wall along an axis perpendicular to the weak plane.

No tensile failure is detected.

In different position the wellbore is in tension at yield point.

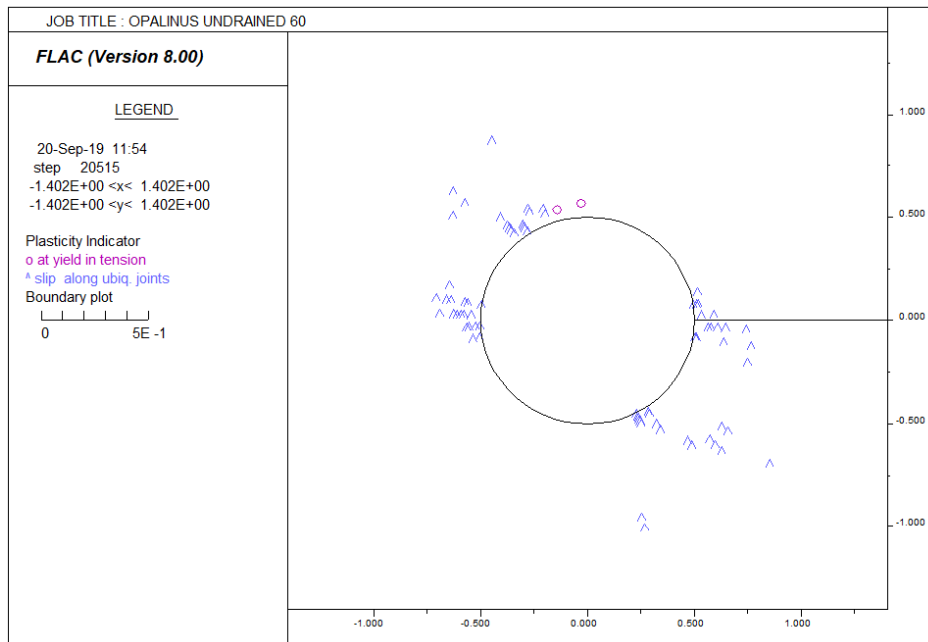


Fig 4.3b: plasticity state after consolidation of the with bedding planes inclined of 60° (obtained from FLAC analysis)

In Fig 4.3 is showed the mechanic response after the simulation of opalinus clay with bedding planes having inclination of 60°.

Here, no tensile failure is detected. The slip along ubiquitous joints is located along an axis perpendicular to the bedding plane inclination, and the breakout of the formation develops symmetrically on both the sides with the same path.

The wellbore wall and, in general, the formation is not in tension in this condition, in the remaining zones where breakout doesn't occur.

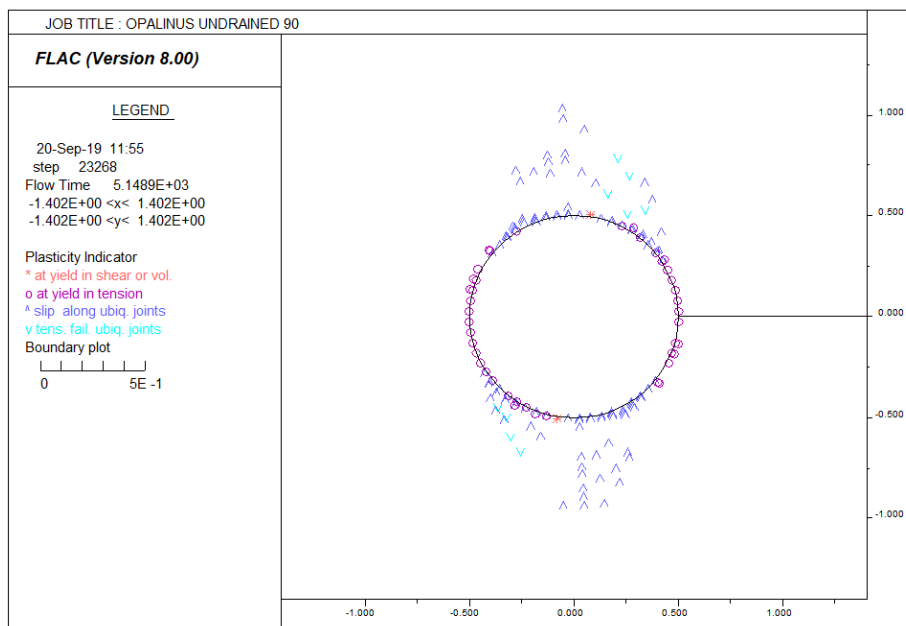


Fig 4.4: plasticity state after consolidation of the with bedding planes inclined of 90° (obtained from FLAC analysis)

In Fig 4.4 is showed the plasticity of the formation. Here, we can see a critical situation.

The blue arrows indicated the slip along ubiquitous joints. The formation breaks and the slip along the joint occurs along planes placed at 0° with respect the direction of bedding planes ($\delta=90^\circ$). The break of the formation is in the same direction of the bedding planes and the minimum far field stress applied (5 MPa) and perpendicular to the maximum far field stress applied (7 MPa).

Along the direction of the minimum far field stress (horizontal) there is the concentration of a tension state, at yield, that anticipates the tensile failure of the formation.

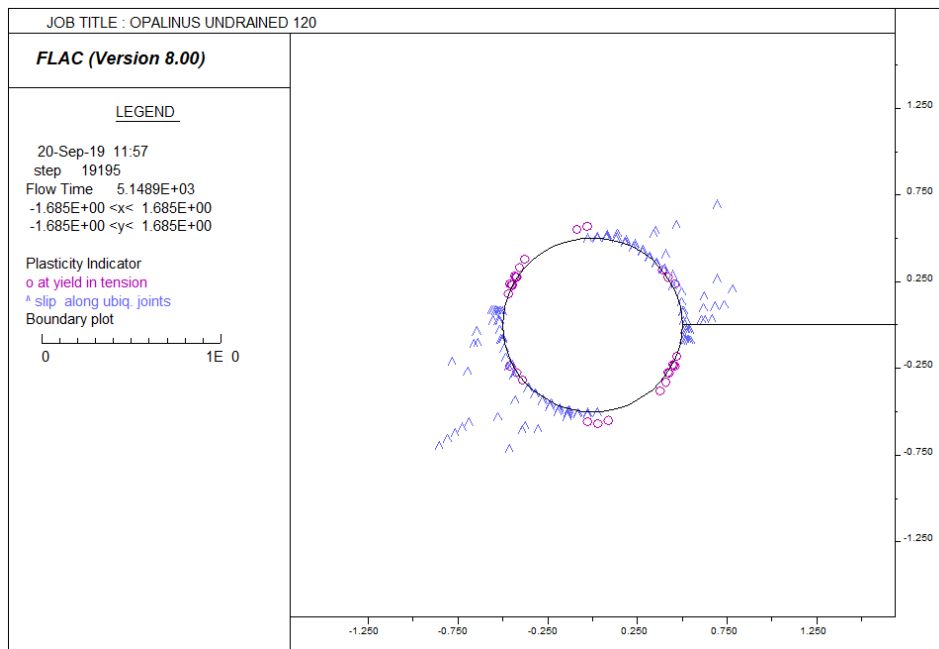


Fig 4.5: plasticity state after consolidation of the with bedding planes inclined of 120° (obtained from FLAC analysis)

Fig 4.5 shows the mechanic response after the simulation of opalinus clay with bedding planes having inclination of 120° .

In Fig 4.5b is showed the plasticity of the formation. The blue arrows indicated the slip along ubiquitous joints. The turquoise arrows indicate the tensile at ubiquitous joints and the violet circles indicate that the formation is at yield in tension.

The formation breaks and the slip (blue arrows) along the joint occurs along planes placed at about 90° clockwise with respect the direction of bedding planes ($\delta=120^\circ$).

The tension state (violet circles), which reaches the yield point, characterizes the remaining perimeter of the wellbore wall.

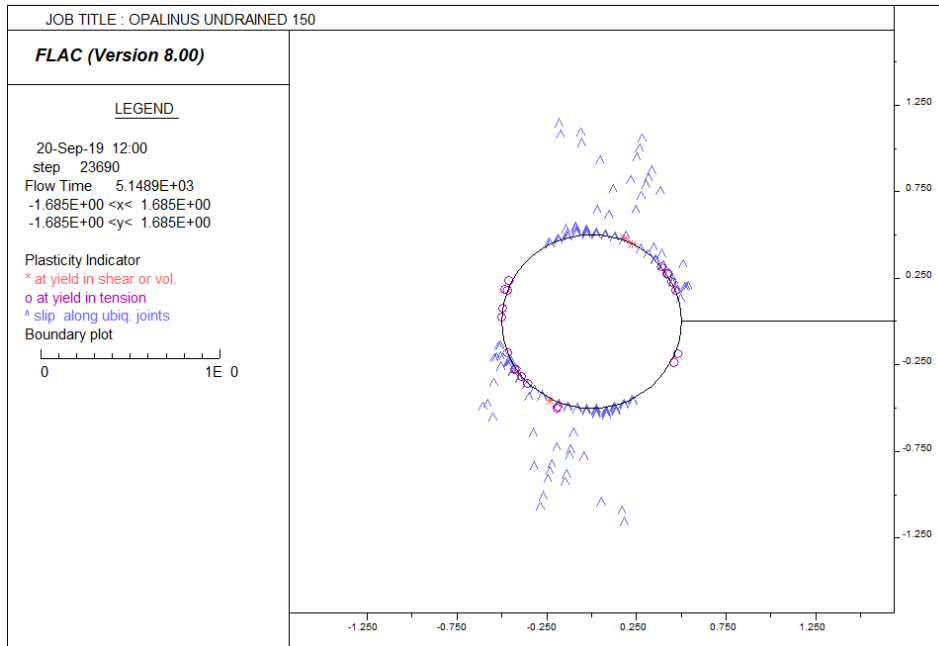


Fig 4.6: plasticity state after consolidation of the with bedding planes inclined of 150° (obtained from FLAC analysis)

In Fig 4.6 is showed the mechanic response after the simulation of opalinus clay with bedding planes having inclination of 150°.

The slip along the joints affects a lot the formation and develops orthogonally with respect to bedding planes (blue arrows) . Perpendicular to the joints slipping, the wellbore is in tension (violet circles).

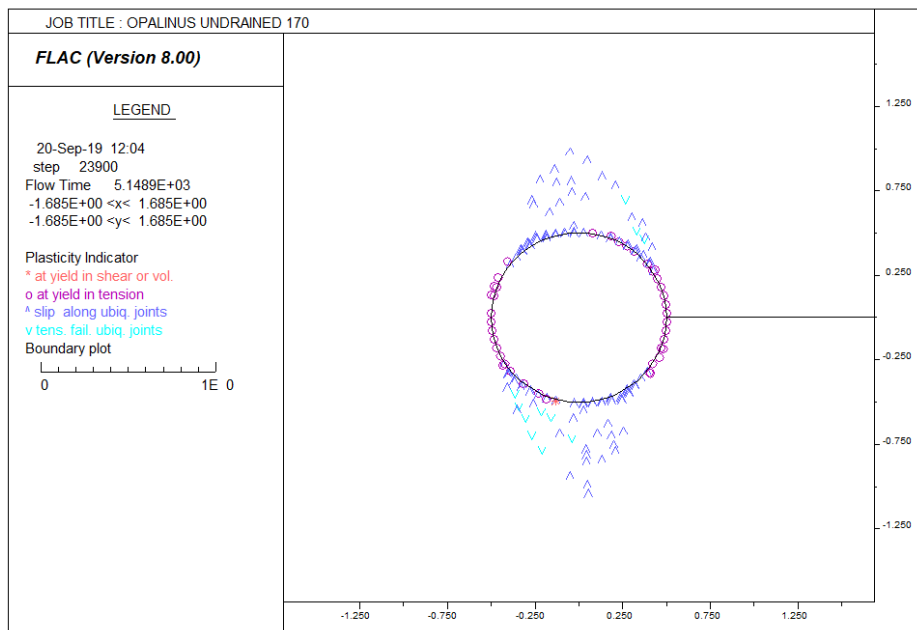


Fig 4.7: plasticity state after consolidation of the with bedding planes inclined of 170° (obtained from FLAC analysis)

In Fig 4.7 is showed the mechanic response after the simulation of opalinus clay with bedding planes having inclination of 170°.

The situation is similar to the 0° inclined bedding planes. The formation breaks and the slip (blue arrows) along the joint occurs orthogonally to the bedding planes direction coupled with the tensile failure (turquoise arrows).

In the same direction of the bedding planes (170°) is concentrated, closer to the wellbore wall, the tension state, at yield. In this direction, it is probably that a failure could also occur, with a consolidation time larger than 5000 seconds.

4.1.2 Drained conditions process simulation

The drained conditions process considers that the pore water of the formation moves. The formation is fully saturated and changes in volume due to the water displacement are considered. For a practical issue, the time of consolidation is set up to 15 days (50000 seconds), because, generally, a drilled hole is then filled by fluids to sustain walls.

Also in this case, the simulation has been repeated with different bedding planes inclination.

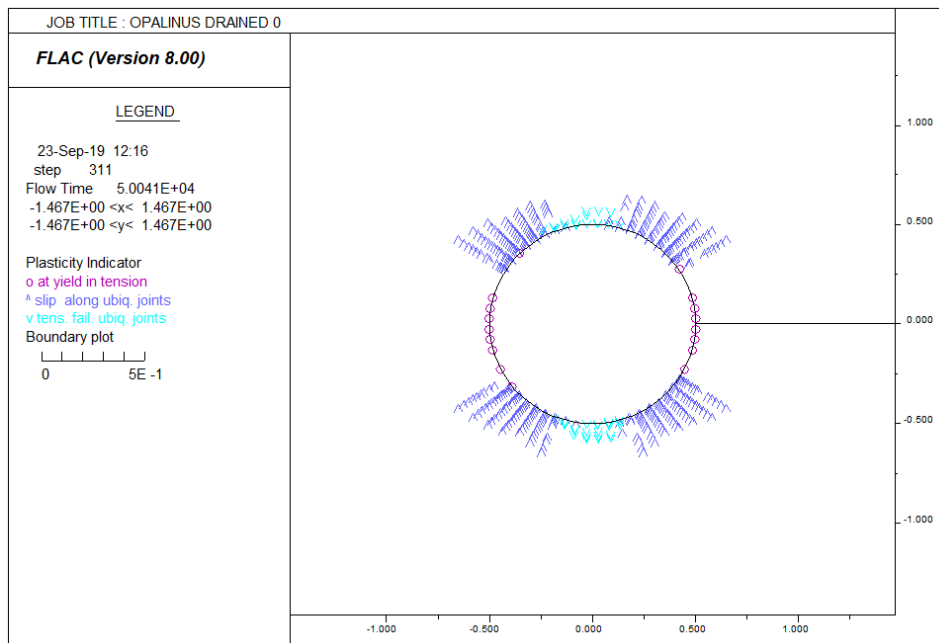


Fig 4.8: plasticity state after consolidation of the with bedding planes inclined of 0° (obtained from FLAC analysis)

For 0° bedding planes, in drained conditions, slip along ubiquitous joints is visualized. The wellbore breaks at 90°, counter-clockwise, from the horizontal direction.

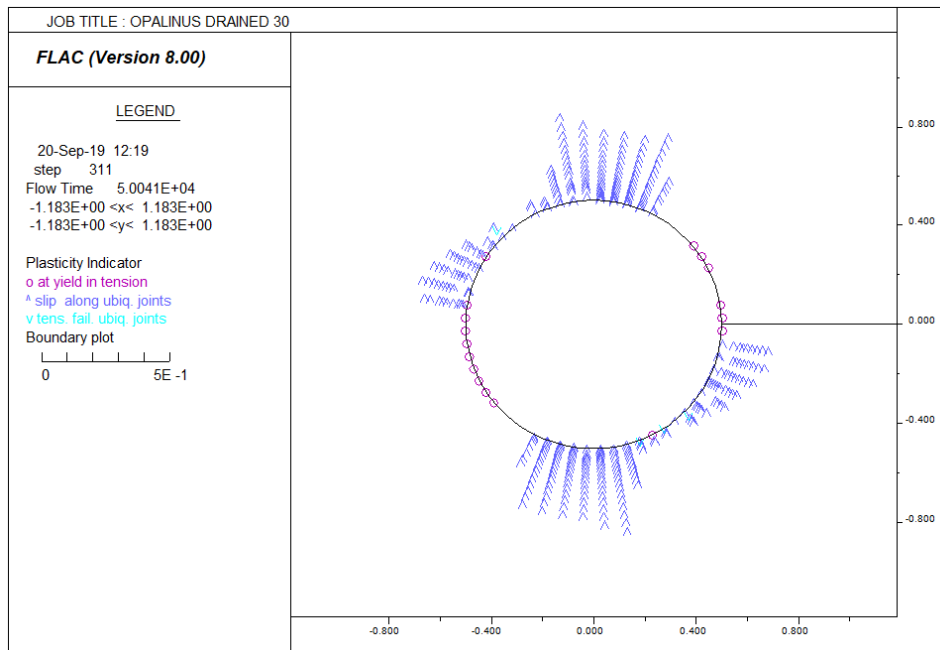


Fig 4.9: plasticity state after consolidation of the with bedding planes inclined of 30° (obtained from FLAC analysis)

Increasing the bedding plane inclination the situation changes. In fig 4.9 is showed what is the influence of 30° weakness plane inclination. We see, a large slip along ubiquitous joints (blue arrows), from 60° to 150° with respect the horizontal direction. The break of the formation develops also far from the wellbore wall. In the zone which are not affected by breakout we can see the tension state (violet circles) which anticipated the failure.

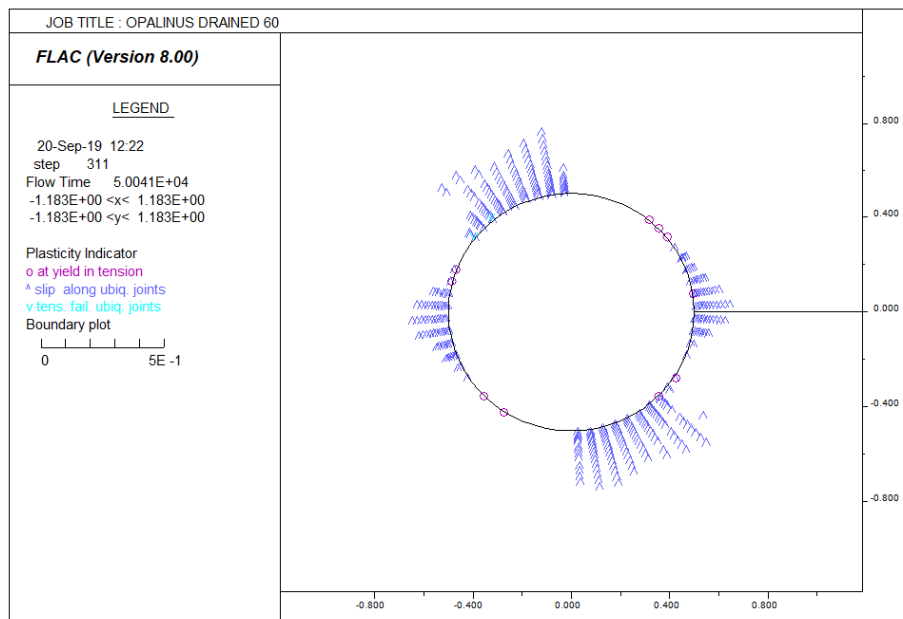


Fig 4.10: plasticity state after consolidation of the with bedding planes inclined of 60° (obtained from FLAC analysis)

In Fig 4.10 is showed the plasticity of the formation when the bedding plane is inclined of 60°.

The blue arrows indicated the slip along ubiquitous joints and it is concentrated along the different axis, one in the horizontal direction (x-direction) and the other at 120° with respect the x axis.

In the direction of the minimum far field stress (5 MPa, x-direction) the amount of formation that breaks is smaller than in the other direction.

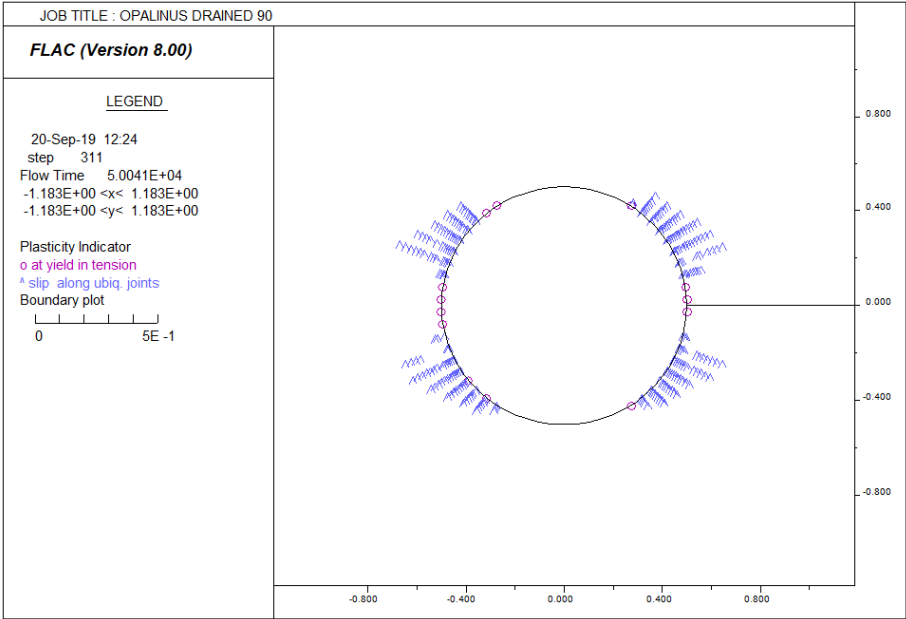


Fig 4.11: plasticity state after consolidation of the with bedding planes inclined of 90° (obtained from FLAC analysis)

Fig 4.11 shows the plasticity of the formation when the bedding plane is inclined of 90°.

The slip along ubiquitous joints develops orthogonally to the bedding planes inclination (blue arrows) which is anticipated by a tension state (violet circles).

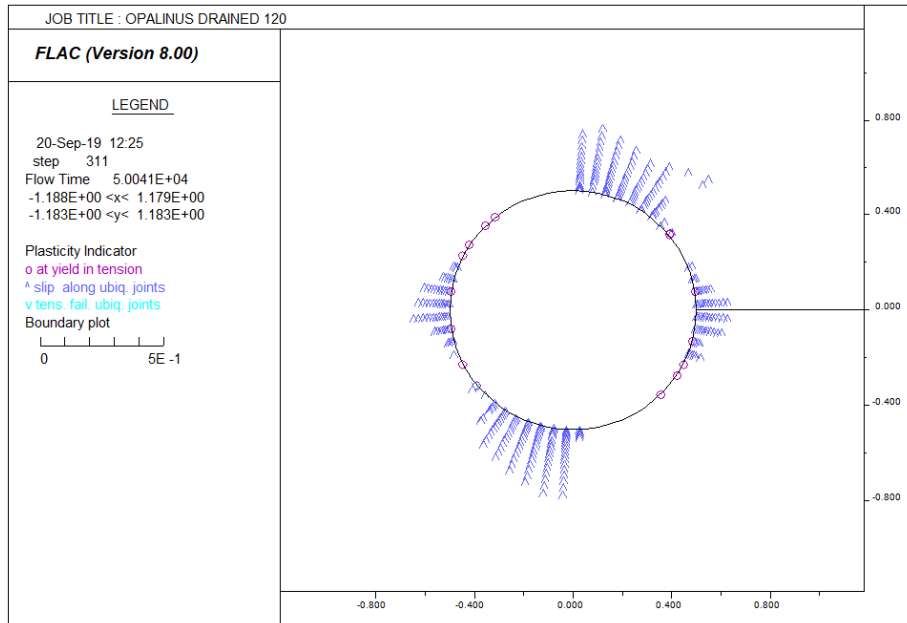


Fig 4.12: plasticity state after consolidation of the with bedding planes inclined of 120° (obtained from FLAC analysis)

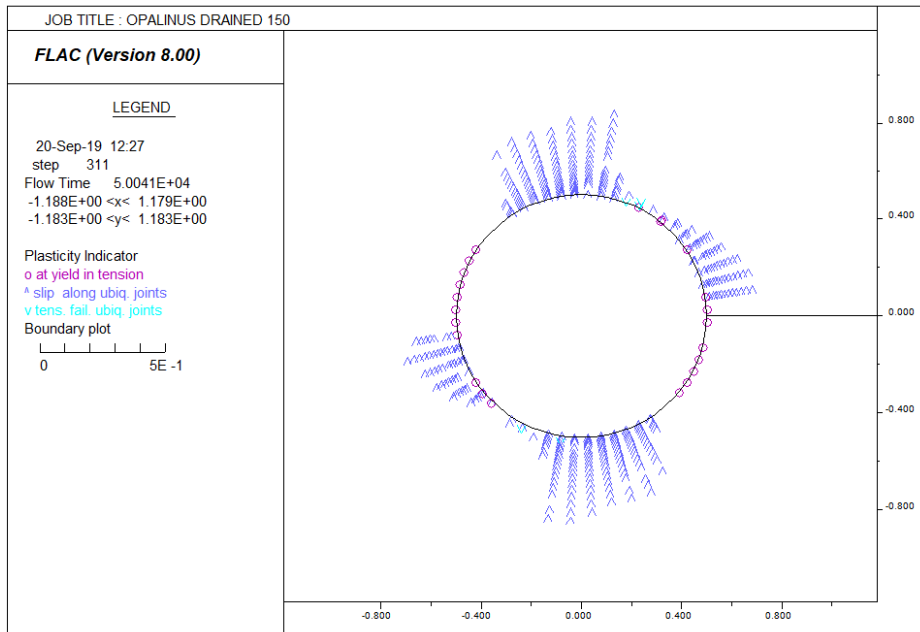


Fig 4.13: plasticity state after consolidation of the with bedding planes inclined of 150° (obtained from FLAC analysis)

Fig 4.12 and fig 4.13 show the development of the breakout in the opalinus shale formation when the inclination pf weakness plane is 120° and 150°, respectively.

From the charts, we can see a similar breakout pattern.

In both the cases, the breakout occurs along an imaginary planes placed at 90° clock-wise from the bedding planes inclination.

And the same for the the case in which the inclination angle of bedding planes is 170° (fig 4.14).

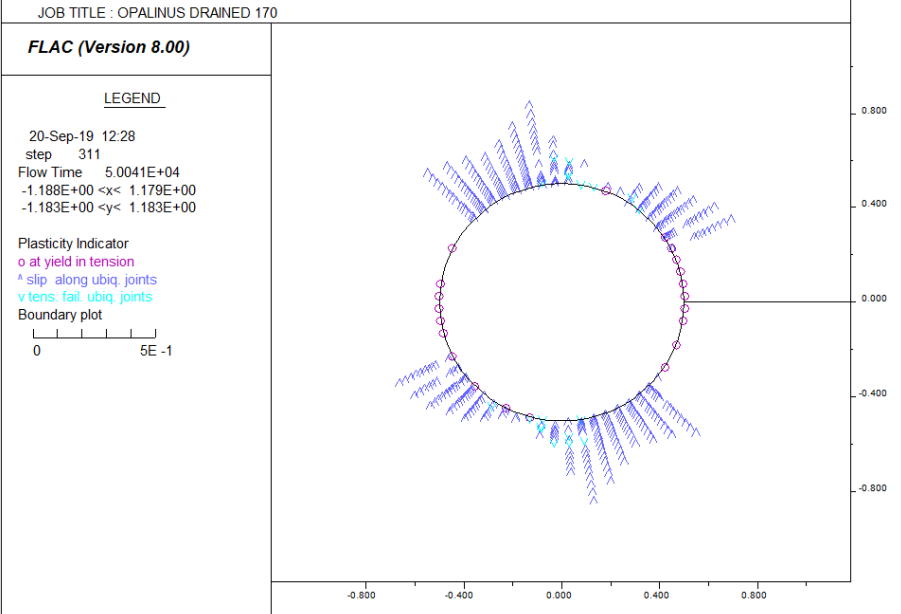


Fig 4.14: plasticity state after consolidation of the with bedding planes inclined of 170° (obtained from FLAC analysis)

4.2 Posedonia Shale Failure Simulation

4.2.1 1 Undrained conditions process after consolidation simulation

The undrained conditions process considers that the pore water of the formation does not move. The formation is fully saturated but no changes in volume are allowed.

Different inclinations (δ) of weakness planes have been implemented, from 0° to 170° (counter-clockwise), and the results from FLAC show how the formation, near the wellbore wall, fails and in which direction the slip of ubiquitous joint occurs.

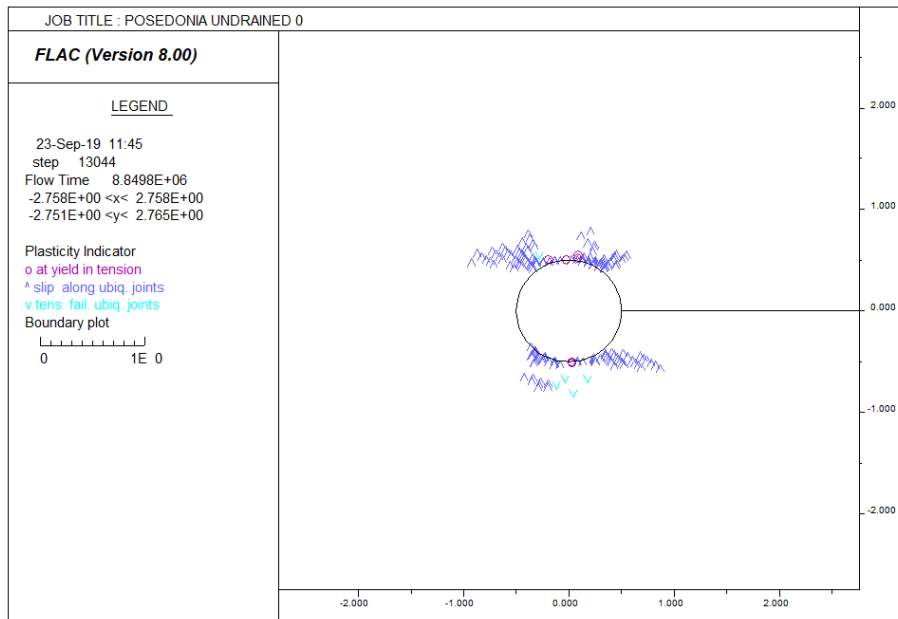


Fig 4.15: plasticity state after consolidation of the with bedding planes inclined of 0° (obtained from FLAC analysis)

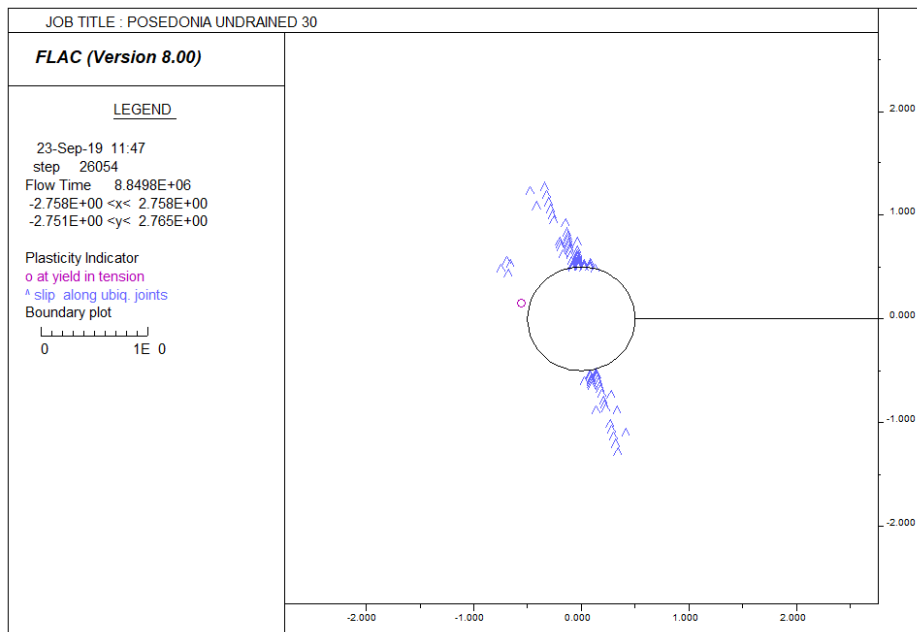


Fig 4.16: plasticity state after consolidation of the with bedding planes inclined of 30° (obtained from FLAC analysis)

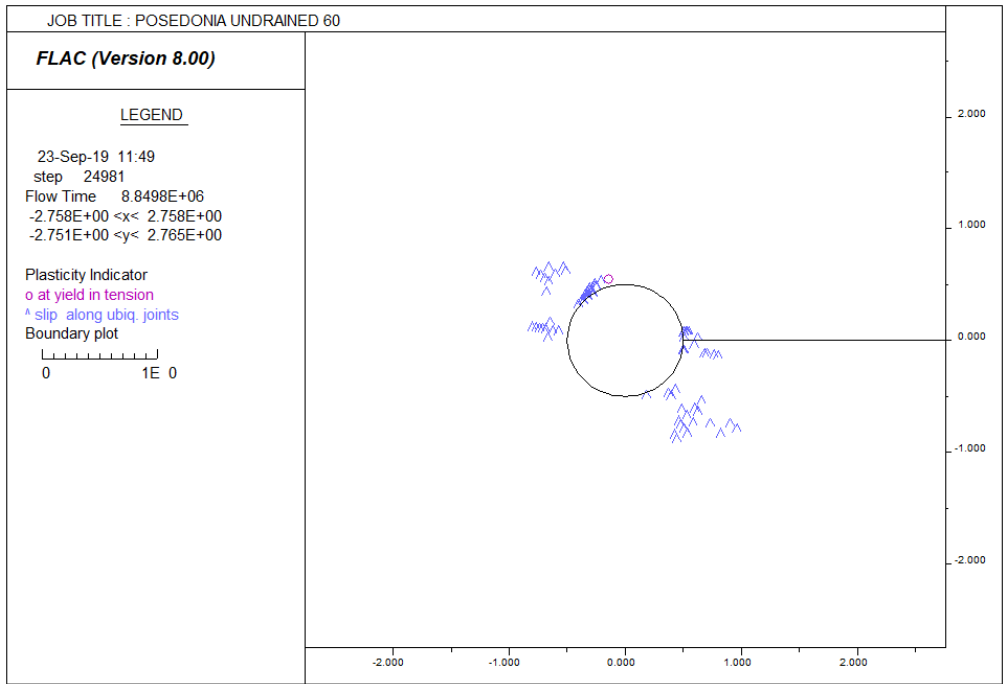


Fig 4.17: plasticity state after consolidation of the with bedding planes inclined of 60° (obtained from FLAC analysis)

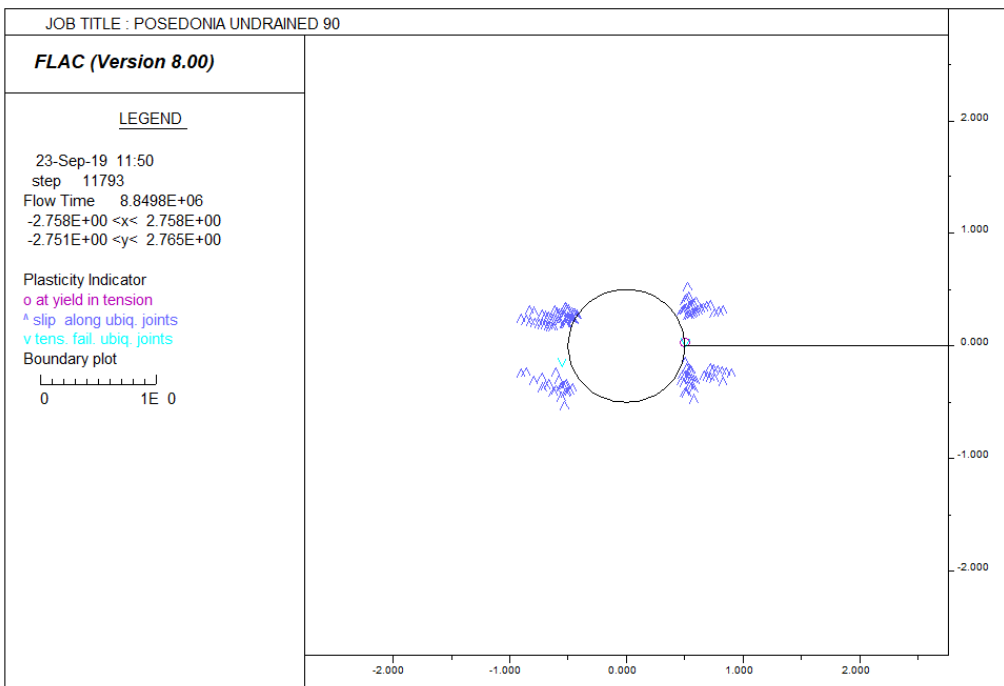


Fig 4.18: plasticity state after consolidation of the with bedding planes inclined of 90° (obtained from FLAC analysis)

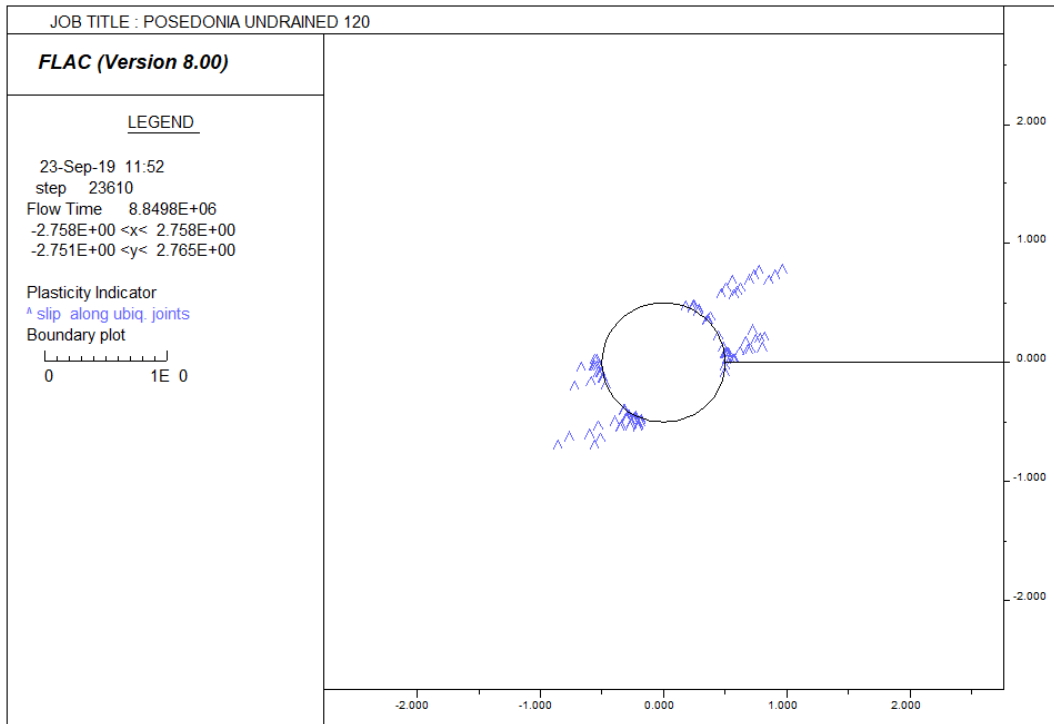


Fig 4.19: plasticity state after consolidation of the with bedding planes inclined of 120° (obtained from FLAC analysis)

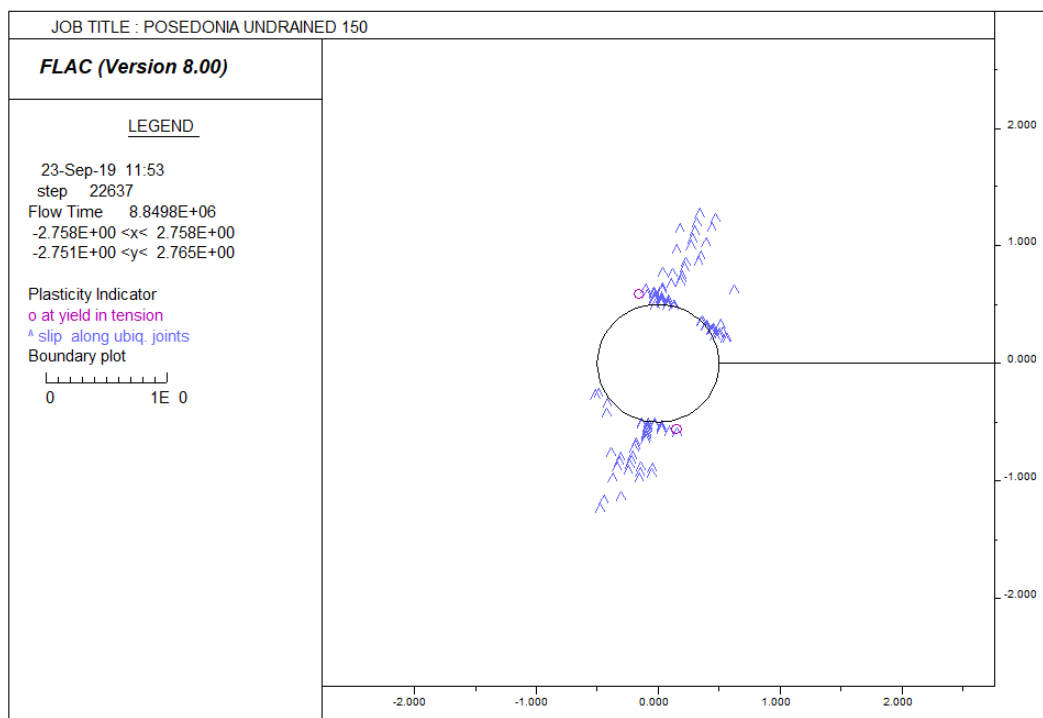


Fig 4.20: plasticity state after consolidation of the with bedding planes inclined of 150° (obtained from FLAC analysis)

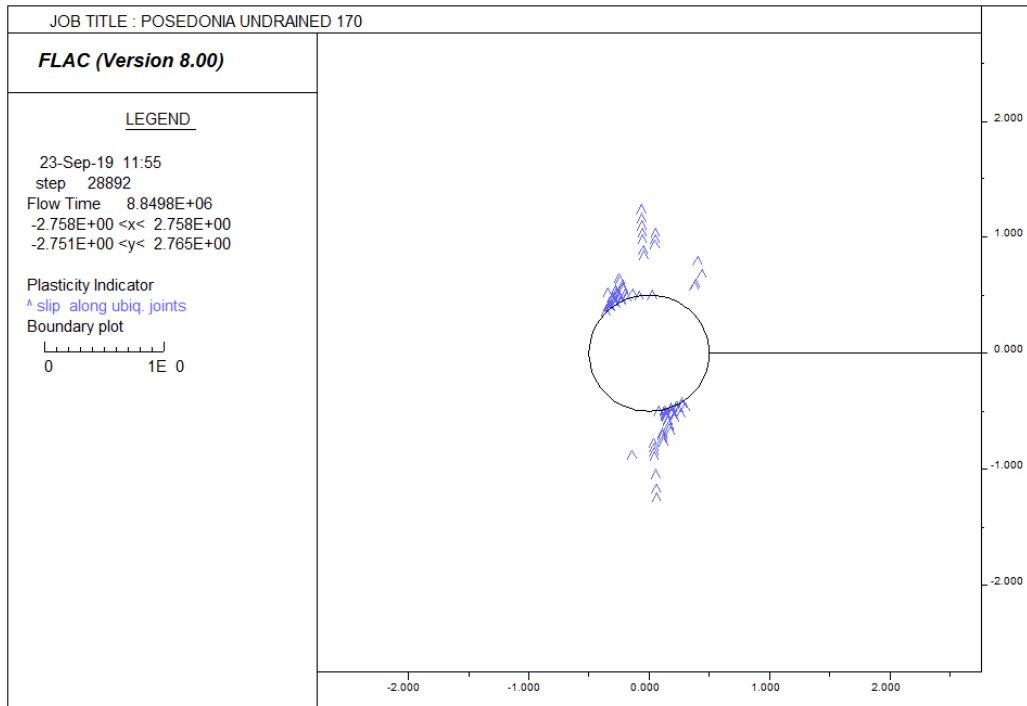


Fig 4.21: plasticity state after consolidation of the with bedding planes inclined of 170° (obtained from FLAC analysis)

Also in this case, we can see the breakout of the formation of the wellbore wall. From fig 4.15 to 4.21 is showed the stability of the wellbore drilled in transversely isotropic material, with bedding planes inclination angle from 0° to 170° .

The simulation takes into account a consolidation time of 50000 s (around 15 days); the consolidation process help us to understand how the formation reacts when, after the simulation, the stresses applied are null.

As we have see for the opalinus clay, also in the posedonia shale the breakout, in the majority of the cases, occurs along a plane placed orthogonally to the bedding plane. And the degrees of breakage is depending, also, on the direction of maximum far field stress applied.

For 0° and 90° , fig 4.15 and 4.18, the failure is confined closer to the wellbore wall.

Far all the other cases, the failure has a larger extension.

4.2.2 Drained conditions process simulation

The drained conditions process considers that the pore water of the formation moves. The formation is fully saturated and changes in volume due to the water displacement are considered

In this case, no change in volume and no breakouts have been retrieved from the simulator (fig 4.22).

So the effect of the pore water makes the wellbore stable.

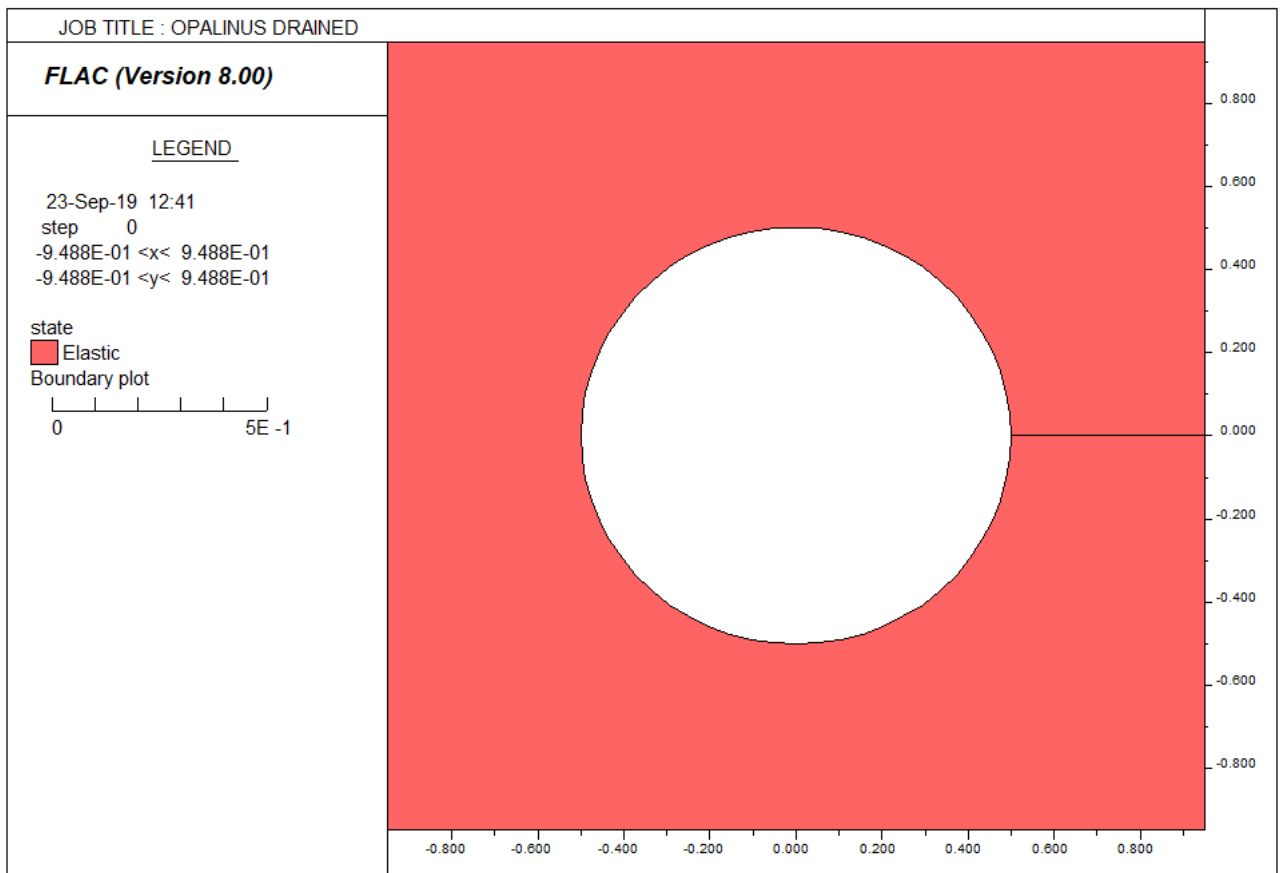


Fig 4.22: plasticity state of formation simulated in drained conditions (obtained from FLAC analysis)

4.3 Discussion of the results

The obtained above results derive from different condition on opalinus clay and posedonia shale:

- Undrained followed by consolidation for both the formation, in anisotropic stress field;
- Drained followed by consolidation for opalinus clay, in anisotropic stress field;
- Drained without consolidation for posedonia shale, in anisotropic stress field;
- Undrained without consolidation for posedonia, in isotropic stress field.

All the different conditions, in which the formation have been analysed, infer the stability of the wellbore except for the posedonia shale in drained condition that does not show plasticization and consequent breakout.

All the plots are useful to understand and predict in which direction the failure develops and the degree of breakage. Generally, from the results, we can see that the breakout occurs, more or less, orthogonally to the bedding planes.

Only the posedonia shale, in isotropic stress field, shows the same breakage pattern for the different bed inclination.

In the scientific literature a lot of scientist have studied the behaviour of rock. Below, the are the comparison between my model and lab tests conducted on opalinus clay and posedonia shale.

The results, obtained during this phase of the simulation, confirms the results obtained by Blumling in 2007 [22, 37]:

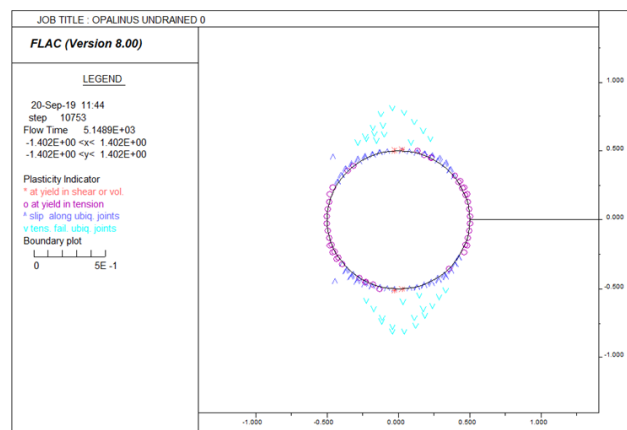
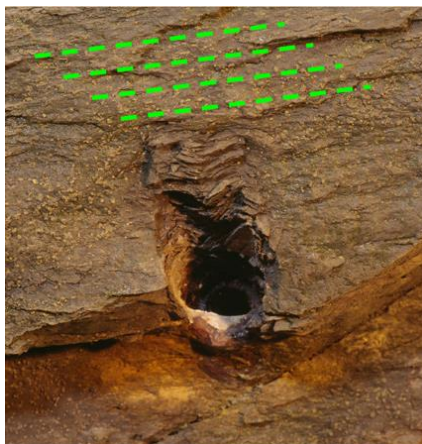


Fig 4.23 excavation in opalinus clay [37] **Fig 4.24** Flac simulation results (from FLAC)

In fig 4.23 is showed the excavation of a hole in the opalinus clay with bedding plane inclination of 0° and the breakout development in the perpendicular plane and fig 4.24 shows the result

of the simulation. The result of Flac code confirms that the model is consistent with the experimental results.

Also for the posedonia shale we can compare the results of a research conducted by Meier in 2004.

Meier [38] analysed some posedonia shale samples characterized by different bedding plane inclination and he obtained the results showed in fig 4.25, while in fig 4.26 there is the result obtained from FLAC for the same situation:

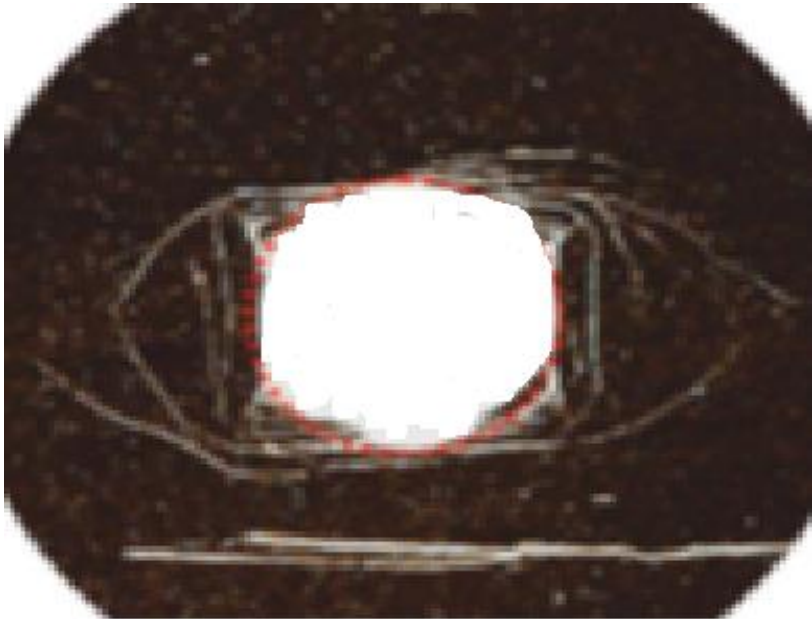


Fig 4.25: Meier result on posedonia sample in isotropic stress field [38]

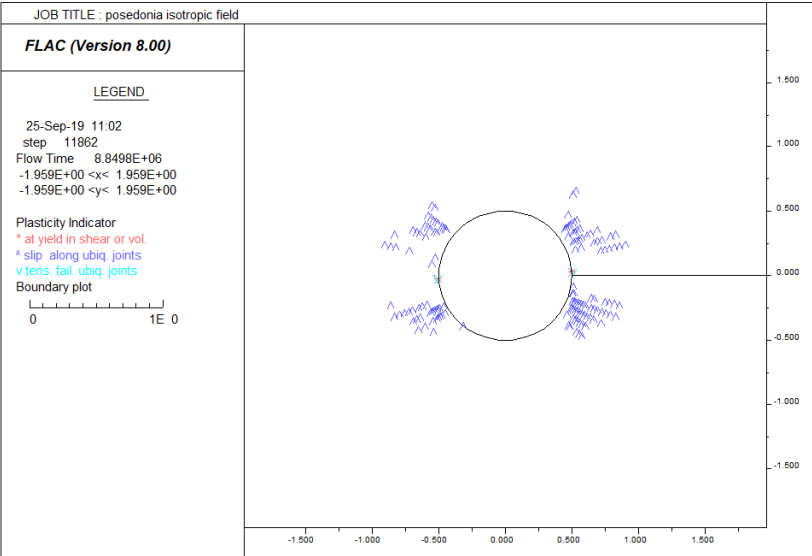


Fig 4.26: FLAC simulation on posedonia shale in isotropic stress far field (from FLAC)

The two different ways to model the wellbore breakout show the same breakage pattern.

5. CONCLUSIONS

The main aim of this thesis is to investigate the stability of formations that could have an interest in the oil and gas field, in particular I have simulated the behaviour of two different kind of rock: the opalinus clay and the posedonia shale.

Both of these formation, from a petroleum geological point of view, could be considered as cap rock or ad unconventional oil or gas reservoirs. But, now day they have been studied because can represent a way to trap radioactive wastes [39] , in fact the two formation in exam have a very low porosity and permeability.

The results obtained are showed in graphical form, in which we can see the presence and the direction of breakout (see section 4).

In general, the study leads to the conclusion that the failure of the rock occurs along planes orthogonally to the bedding planes and the degrees of these failures depended on the stress applied and on the pore water flowing mechanism.

In the simulation of the undrained opalinus clay, the breakout is more or less shaped symmetrically and regular.

Comparing Flac results with lab tests and in situ tests, it can be said that the simulation can represent a good tools to analyse stability (see section 4.3) of wellbore in different type of formation; obviously, the non perfect match between the experimental result and theoretical one will not match perfectly because of the uncertainties of the implemented petrophysical parameters of the formation, which is considered uniform unless for the presence of weakness planes.

APPENDIX A: FLAC code for undrained condition followed by consolidation for opalinus clay

```
def donut
  command
    grid ize,jze
    model elastic
  end_command
  ki=(rmin*rmul-rmin)/(gratio^ize-1.0)
  kj=deltaangle*pi/180.0/jze
  kj0=minangle*pi/180.0;
  loop j (1,jgp)
    alfa=kj0+(j-1)*kj
    sina=sin(alfa)
    cosa=cos(alfa)
    rp=1.0
    loop i (1,igp)
      ro=rmin+ki*(rp-1.0)
      x(i,j)=xcenter+ro*cosa
      y(i,j)=ycenter+ro*sina
      rp=rp*gratio
    end_loop
  end_loop
  figp=ize+1
  fjgp=jze+1
  if abs(deltaangle-360.0)<1e-4 then
    command
      attach aside from 1,1 to figp,1 bside from 1,fjgp to figp,fjgp
    end_command
  end_if
end
set rmin=0.5 rmul=40.0 gratio=1.1 xcenter=0.0 ycenter=0.0 ize=60
```

```

set jzone=60 minangle=0 deltaangle=360
donut
group 'User:sandstone'
model ubi group 'User:sandstone'
prop density=2400.0 bulk=8.7E9 shear=4.4E9 cohesion=5e6 friction=24 tension=1.2e6
dilation=0
prop jangle=0 jcohesion=1e6 jfriction=21 jdilation=0 jtension=0.3e6 group 'User:sandstone'
prop porosity=0.2
prop perm=1e-17
water density=1000 bulk=2e9 tens 10e10
;
ini sat=1
fix sat
;
ini pp 2e6
;
ini sxx -7e6 ;-3e6
ini syy -5e6 ;-7e6
ini szz -6e6
;fix pp0 ; cd
apply sxx -7e6 from 61,1 to 61,61
apply syy -5e6 from 61,1 to 61,61
;apply pressure 2.5e6 from 1,1 to 1,61
set mech on flow off
;
his xvel
his yvel
his unbalanced
;
solve elastic
;
;

```

```

def evals
loop i (1,izones)
loop j (1,jzones)
temp1=.5*(sxx(i,j)+syy(i,j))
temp2=sqrt(sxy(i,j)^2+.25*(sxx(i,j)-syy(i,j))^2)
;stm=temp1-temp2
ex_4(i,j)=temp1-temp2
;srm=temp1+temp2
ex_5(i,j)=temp1+temp2
end_loop
end_loop
end
set mech on flow on
hist pp i=1 j=16
hist pp i=1 j=12
hist pp i=1 j=5
hist pp i=1 j=8
his unbal
ini pp 0e6 i=1
fix pp i=1
fix pp i=61 j 1 61
;set nmech=10
solve auto on age 5000

```

APPENDIX B: FLAC code for drained condition followed by consolidation process for opalinus clay

```
def donut
  command
    grid ize,jze
    model elastic
  end_command
  ki=(rmin*rmul-rmin)/(gratio^ize-1.0)
  kj=deltaangle*pi/180.0/jze
  kj0=minangle*pi/180.0;
  loop j (1,jgp)
    alfa=kj0+(j-1)*kj
    sina=sin(alfa)
    cosa=cos(alfa)
    rp=1.0
    loop i (1,igp)
      ro=rmin+ki*(rp-1.0)
      x(i,j)=xcenter+ro*cosa
      y(i,j)=ycenter+ro*sina
      rp=rp*gratio
    end_loop
  end_loop
  figp=ize+1
  fjgp=jze+1
  if abs(deltaangle-360.0)<1e-4 then
    command
      attach aside from 1,1 to figp,1 bside from 1,fjgp to figp,fjgp
    end_command
  end_if
end
set rmin=0.5 rmul=40.0 gratio=1.1 xcenter=0.0 ycenter=0.0 ize=60
```

```

set jzone=60 minangle=0 deltaangle=360
donut
group 'User:sandstone'
model ubi group 'User:sandstone'
prop density=2400.0 bulk=8.6E9 shear=4.4E9 cohesion=5e6 friction=24 tension=1.2e6
dilation=0
prop jangle=0 jcohesion=1e6 jfriction=21 jdilation=0 jtension=0.3e6 group 'User:sandstone'
prop porosity=0.2
prop perm=1e-17
water density=1000 bulk=2e9 tens 10e10
;
ini sat=1
fix sat
;
ini pp 2e6
;
ini sxx -7e6 ; -3e6
ini syy -5e6 ; -7e6
ini szz -6e6
;fix pp0 ; cd
apply sxx -7e6 from 61,1 to 61,61
apply syy -5e6 from 61,1 to 61,61
;apply pressure 2.5e6 from 1,1 to 1,61
set mech on flow on
;
his xvel
his yvel
his unbalanced
;
;> solve elastic
; *** Solve Elastic not applicable or interrupted.
set mech on flow on

```

```
hist pp i=1 j=16
hist pp i=1 j=12
hist pp i=1 j=5
hist pp i=1 j=8
his unbal
ini pp 0e6 i=1
fix pp i=1
fix pp i=61 j 1 61
;set nmech=10
solve auto on age 50000
```

REFERENCES

- [1] Fjaer E., Holt R.M., Horsrud P., Raaen A.M., Risnes R., "Petroleum related rock mechanics", 2008
- [2] Kelly, "Solid Mechanics Part II"
- [3] Hoek E., Brown E.T., "The Hoek- Bron failure criterion and GSI", 2018
- [4] Rocscience website, "Generalized Hoek-Brown Criterion", 2002
- [5] Lang J., "Transversely isotropic specimen with bedding/weak plane in triaxial compressive", 2011
- [6] <https://www.instructables.com/id/Steps-to-Analyzing-a-Materials-Properties-from-its/>
- [7] <https://brilliant.org/wiki/cylindrical-coordinates/>
- [8] https://www.researchgate.net/figure/Breakout-and-cavings-due-to-failure-along-plane-of-weakness-Source-Chris-Gallant-et_fig3_267459764
- [9] <https://kks32-slides.github.io/2018-effective-stress/>
- [10] <https://link.springer.com/article/10.1007/s00419-017-1318-x>
- [11] https://en.wikipedia.org/wiki/Mohr%27s_circle
- [12] <http://www.iue.tuwien.ac.at/phd/singulani/dissu4.html>
- [13] Staab G.H., "Laminar Composites", 1999
- [14] Staab G.H., "Laminar Composites", 2015
- [15] Buiocchi F., Adamowski J.C. , "Comprehensive Materials Processing" , 2014
- [16] FLAC Manual
- [17] Deangeli C., Omwanghe O.O., "Prediction of mud pressures for the stability of wellbores drilled in transversely isotropic rocks", 2018
- [18] Rohol H.J., Schmid-Rohl A., Oschmann W., Frimmel A., Schwark L., "The Posidonia Shale (Lower Toarcian) of SW-Germany: an oxygen-depleted ecosystem controlled by sea level and palaeoclimate", 2001
- [19] Van Bergen F., Zijp M., Nelskamp S., Kombrink H., "Shale gas evaluation of the early Jurassic Posidonia Shale formation and the Carboniferous Epen Formation in the Netherlands", 2013
- [20] https://www.researchgate.net/publication/236574149_Hydrocarbon_habitat_of_the_West_Netherlands_Basin
- [21] Meier T., "Borehole breakouts in transversely isotropic Posidonia Shale", 2017
- [22] Popp T., Salzer K., "Anisotropy of seismic and mechanical properties of Opalinus clay during triaxial deformation in a multi-anvil apparatus", 2006

- [23] Esemé E., Urai J.L., Krooss B.M., Littke R., “Review of mechanical properties Of oil shale: implications for exploitation and basin modelling”, 2007
- [24] Grathoff G.H., Peltz M., Enzmann F., Kaufhold S., “Porosity and permeability determination of organic-rich Posidonia shales based on 3-D analyses by FIB-SEM microscopy”, 2016
- [25] Bossart P., “Characteristics of the opalinus clay at Mont Terri”, 2005
- [26] Forge report D4.6, “Review of Boom Clay and Opalinus Clay parameters”, 2010
- [27] Bock H., “RA Experiment: Updated review of the rock mechanics properties of the Opalinus Clay of the Mont Terri URL based on laboratory and Fiel Testing “, 2009
- [28] Amann F., Vogelhuber M., “Assessment of geomechanical properties of intact opalinus clay”, 2015
- [29] Corkum A.G., Martin C.D., “The mechanical behaviour of weak mudstone (Opalinus Clay) at low stresses” 2006
- [30] Forge report D4.6, “Review of Boom Clay and Opalinus Clay parameters”, 2010
- [31] Graslé W., “Multistep triaxial strength tests: investigating strength parameters and pore pressure effects on opalinus clay”, 2011
- [32] Amann F., Kaiser P., Button E.A., “Experimental study of Brittle behavior of clay shale in rapid triaxial compression”, 2011
- [33] Morgan S.P., Einstein H.H., “The effect of bedding plane orientation on crack propagation and coalescence in shale”, 2014
- [34] Hunsche U., Walter F., Schnier H., “Evolution and failure of the Opalinus clay: relationship between deformation and damage, experimental results and constitutive equation”, 2004
- [35] Chang L., Konietzky H., “Application of the Mohr-Coulomb Yield criterion for rocks with multiple joint sets using fast Lagrangian analysis of continua 2D (FLAC2D) software”, 2018
- [36] Gang L., Hong L., Harumi K., Mizuka Y., “Application of ubiquitous joint model in numerical modeling of Hilltop mines in Japan”, 2003
- [37] Blumling P., Bernier F., Lebon P., Martin C.D., “The excavation damaged zone in clay formations time-dependent behaviour and influence on performance assessment”, 2006
- [38] Meier T., Rybacki E., Backers T., Dresen G., “Influence of bedding angle on borehole stability: A laboratory investigation of transverse isotropic oil shale”, 2014
- [39] Amann F., Martin C.D., Thoeny R., “Rock mechanical considerations associated with the construction of deep nuclear waste disposal in clay rock”, 2012

